

## Colorectal cancer: Parametric evaluation of morphological, functional and molecular tomographic imaging

Pier Paolo Mainenti, Arnaldo Stanzione, Salvatore Guarino, Valeria Romeo, Lorenzo Ugga, Federica Romano, Giovanni Storto, Simone Maurea, Arturo Brunetti

**ORCID number:** Pier Paolo Mainenti (0000-0003-3592-808X); Arnaldo Stanzione (0000-0002-7905-5789); Salvatore Guarino (0000-0003-3978-2567); Valeria Romeo (0000-0002-1603-6396); Lorenzo Ugga (0000-0001-7811-4612); Federica Romano (0000-0003-0685-0201); Giovanni Storto (0000-0002-6168-5598); Simone Maurea (0000-0002-8269-3765); Arturo Brunetti (0000-0001-7057-3494).

**Author contributions:** All authors equally contributed to this paper with conception and design of the study, literature review and analysis, drafting and critical revision and editing, and final approval of the final version.

**Conflict-of-interest statement:** No potential conflicts of interest. No financial support.

**Open-Access:** This article is an open-access article which was selected by an in-house editor and fully peer-reviewed by external reviewers. It is distributed in accordance with the Creative Commons Attribution Non Commercial (CC BY-NC 4.0) license, which permits others to distribute, remix, adapt, build upon this work non-commercially, and license their derivative works on different terms, provided the original work is properly cited and the use is non-commercial. See: <http://creativecommons.org/licenses/by-nc/4.0/>

**Manuscript source:** Invited manuscript

**Pier Paolo Mainenti**, Institute of Biostructures and Bioimaging of the National Council of Research (CNR), Naples 80145, Italy

**Arnaldo Stanzione, Salvatore Guarino, Valeria Romeo, Lorenzo Ugga, Federica Romano, Simone Maurea, Arturo Brunetti**, University of Naples "Federico II", Department of Advanced Biomedical Sciences, Naples 80131, Italy

**Giovanni Storto**, IRCCS-CROB, Referral Cancer Center of Basilicata, Rionero in Vulture 85028, Italy

**Corresponding author:** Pier Paolo Mainenti, MD, Academic Research, Doctor, Institute of Biostructures and Bioimaging of the National Council of Research (CNR), Naples 80145, Italy. [pierpamainenti@hotmail.com](mailto:pierpamainenti@hotmail.com)

**Telephone:** +39-347-1873089

**Fax:** +39-081-5457081

### Abstract

Colorectal cancer (CRC) represents one of the leading causes of tumor-related deaths worldwide. Among the various tools at physicians' disposal for the diagnostic management of the disease, tomographic imaging (*e.g.*, CT, MRI, and hybrid PET imaging) is considered essential. The qualitative and subjective evaluation of tomographic images is the main approach used to obtain valuable clinical information, although this strategy suffers from both intrinsic and operator-dependent limitations. More recently, advanced imaging techniques have been developed with the aim of overcoming these issues. Such techniques, such as diffusion-weighted MRI and perfusion imaging, were designed for the "*in vivo*" evaluation of specific biological tissue features in order to describe them in terms of quantitative parameters, which could answer questions difficult to address with conventional imaging alone (*e.g.*, questions related to tissue characterization and prognosis). Furthermore, it has been observed that a large amount of numerical and statistical information is buried inside tomographic images, resulting in their invisibility during conventional assessment. This information can be extracted and represented in terms of quantitative parameters through different processes (*e.g.*, texture analysis). Numerous researchers have focused their work on the significance of these quantitative imaging parameters for the management of CRC patients. In this review, we aimed to focus on evidence reported in the academic literature regarding the application of parametric imaging to the diagnosis, staging and prognosis of CRC while discussing future perspectives and present limitations. While the transition from

**Received:** June 18, 2019  
**Peer-review started:** June 20, 2019  
**First decision:** July 22, 2019  
**Revised:** August 6, 2019  
**Accepted:** August 24, 2019  
**Article in press:** August 24, 2019  
**Published online:** September 21, 2019

**P-Reviewer:** Caputo D, Gavriilidis P, Jeong KY, Tchilikidi KY  
**S-Editor:** Gong ZM  
**L-Editor:** A  
**E-Editor:** Ma YJ



purely anatomical to quantitative tomographic imaging appears achievable for CRC diagnostics, some essential milestones, such as scanning and analysis standardization and the definition of robust cut-off values, must be achieved before quantitative tomographic imaging can be incorporated into daily clinical practice.

**Key words:** Colorectal cancer; Computed tomography; Magnetic resonance imaging; Positron emission tomography; Parametric imaging; Perfusion imaging; Diffusion imaging; Texture analysis

©The Author(s) 2019. Published by Baishideng Publishing Group Inc. All rights reserved.

**Core tip:** While encouraging progress has been made in the management of colorectal cancer (CRC), it still remains among the malignancies with higher incidence and mortality. Tomographic imaging plays a crucial role in the diagnosis, staging and evaluation of treatment responses in CRC; however, it may also conceal critical information that could guide treatment decisions. The quantitative analysis of computed tomography (CT), magnetic resonance imaging and positron emission tomography/CT images could unveil novel promising biomarkers in the form of numerical parameters. These parameters, if validated in terms of their clinical significance, may contribute to redefining the role of diagnostic imaging and improving CRC management.

**Citation:** Mainenti PP, Stanzione A, Guarino S, Romeo V, Uggia L, Romano F, Storto G, Maurea S, Brunetti A. Colorectal cancer: Parametric evaluation of morphological, functional and molecular tomographic imaging. *World J Gastroenterol* 2019; 25(35): 5233-5256  
**URL:** <https://www.wjgnet.com/1007-9327/full/v25/i35/5233.htm>  
**DOI:** <https://dx.doi.org/10.3748/wjg.v25.i35.5233>

## INTRODUCTION

Colorectal cancer (CRC) is one of the malignancies with the highest incidence in Western countries and is the third most common cancer in both men and women<sup>[1]</sup>. The TNM staging classification of CRC, based on the depth of tumor invasion (T), lymph node involvement (N) and metastatic spread (M), is strongly associated with the 5-year survival rate<sup>[2]</sup>. Therefore, the timely identification of CRC represents a critical step to prevent the growth of invasive neoplasms. Similarly, accurate preoperative staging is necessary to differentiate CRCs with a good prognosis from those with a poor prognosis to select the most appropriate treatment and to optimize outcomes.

Currently, various imaging modalities are recommended for the clinical evaluation of patients affected by CRC for diagnosis, characterization (differentiation between mucinous and nonmucinous tumors), staging (depth of tumor spread, extramural vascular invasion, and the presence of malignant lymph nodes and distant metastasis), surgical planning (circumferential resection margin and sphincteric involvement in rectal cancer), the assessment of posttreatment tumor responses and follow-up after therapy<sup>[3-5]</sup>. Among these, computed tomography (CT), magnetic resonance imaging (MRI) and 18F-fluorodeoxyglucose (18FDG) positron emission tomography (PET) associated with CT (18FDG-PET/CT) or MRI (18FDG-PET/MRI) play a crucial role in the management of CRC. Qualitative evaluation represents the conventional approach to the use of these imaging modalities

The growth of CRC is accompanied by the activation of numerous biological processes, such as neoangiogenesis and anarchic cellular proliferation, and an increase in cellular energy metabolism and glucose consumption. These processes determine neoplastic heterogeneity, which is characterized by a misshapen, irregular and disorganized tissue architecture with areas of high cell density, hypoxia, necrosis, hemorrhage and myxoid changes. Intratumor heterogeneity tends to change over time and to increase as tumors grow, impacting local and distant neoplastic invasion, the delivery of chemotherapeutic agents, cellular resistance to chemotherapy and radiotherapy and, consequently, prognosis<sup>[6]</sup>.

The current state-of-the-art CT, MRI, and hybrid PET scanners offer the possibility to obtain structural, functional and molecular information about these biological

neoplastic processes. Their “*in vivo*” quantitative evaluation can add value to the diagnostic management of CRC in different clinical settings. Parametric analysis (PA) allows the extraction of the numerical data contained in the voxels of each image and information regarding their processing in terms of parametric maps, parameter distributions, and the quantification of spatial complexity and density, signal intensity or activity for CT, MRI or PET, respectively, by using time curves and volumetry<sup>[7-9]</sup>. PA requires the drawing of a region of interest (ROI) that includes the target tissue for analysis. Depending on the imaging modalities and techniques used, it is possible to obtain different quantitative parameters that are representative of peculiar neoplastic features such as perfusion, structural heterogeneity, cellularity, oxygenation and glucose consumption.

The present review describes the role of imaging PA in patients with CRC by focusing on its technical features, clinical advantages and limitations in advanced quantitative functional and molecular imaging, such as diffusion-weighted MRI (DWI), perfusion imaging (PI), blood oxygenation level-dependent (BOLD) MRI, MR spectroscopy (MRSI) and metabolic imaging as well as advanced quantitative image analysis techniques, such as texture analysis (TA) and volumetry.

## LIMITATIONS OF THE CONVENTIONAL QUALITATIVE ASSESSMENT OF MORPHOLOGICAL IMAGING

The evaluation of images based on morphological features represents the routine clinical approach to CT and MRI. Although this diagnostic approach is recommended in clinical guidelines for the management of CRC, it suffers from several limitations, as shown in [Table 1](#). In particular, the Response Evaluation Criteria in Solid Tumors (RECIST) have been introduced for standardizing the assessment of tumor responses to cytotoxic chemotherapy, and they are mainly based on tumor size measurements<sup>[10]</sup>. However, it has been observed that RECIST can underestimate both responses to chemotherapy (alone or coupled with antiangiogenic agents) and focal therapies<sup>[8,11-13]</sup>. Indeed, solid tumors may respond to therapies by developing intratumoral necrotic areas and/or cystic or myxoid degeneration; as a result, the overall size of the neoplasm may be reduced, unchanged or paradoxically increased<sup>[12,14,15]</sup>.

To overcome the above-described limitations, parametric imaging could be a useful tool to integrate the information obtained from morphological imaging. PA allows the extraction of numerical data as either quantitative parameters (processed according to a pharmacokinetic model and expressed as an absolute amount with a corresponding unit of measurement) or as semiquantitative parameters (as a ratio of the measured amount and a standard of reference and expressed as pure number). In the following text, for the sake of simplicity, we will use the term quantitative to indicate both quantitative and semiquantitative parameters.

## ADVANCED QUANTITATIVE FUNCTIONAL AND MOLECULAR IMAGING

### *Physiological aspects and technical features*

**DWI with apparent diffusion coefficient maps:** DWI is a functional MR technique that measures the Brownian motion of water molecules in biological tissues, which is restricted by an increase in cellularity and architectural tissue changes<sup>[16,17]</sup>. Consequently, water diffusion properties are altered in tumors because of the coexistence of dense cellularity, fibrosis, necrosis, neovascularization and hemorrhage. In detail, the increased tissue cellularity observed in the solid part of a tumor reduces the intercellular space and consequently restricts Brownian motion. By using DWI, it is possible to calculate a quantitative measure of water molecule diffusion over time, known as the ADC. The apparent diffusion coefficient (ADC) value is expressed as  $10^{-3}$  mm<sup>2</sup>/s and can be calculated for each unit volume (voxel) to provide a parametric ADC map. In particular, ADC has been shown to be inversely related to tumor cellularity, and it has been clinically applied to distinguish benign from malignant tumors, to assess tumor grade, to delineate the extent of a tumor, to define the classes of risk that influence the prognosis, and to evaluate and predict tumor treatment responses in CRC patients<sup>[18,19]</sup> ([Figure 1](#)).

**PI based on dynamic contrast enhanced CT or MRI:** Neoangiogenesis, a process induced by the upregulation of vascular growth factors, is a well-known critical aspect of CRC that leads to the development of a new, altered and immature microcirculatory network inside the tumor<sup>[20-22]</sup>. In particular, neoangiogenesis

**Table 1** Current limitations of qualitative imaging based on morphological features used for the assessment of colorectal cancer

Diagnostic task	Limits of qualitative imaging
Primary tumor identification	Early stages of CRC hard to detect Neoplastic and inflammatory tissue not easily differentiable
Lymph node involvement	Lymph node size criteria often misleading and insufficient Shape, border irregularity and structural heterogeneity hard to assess for small lymph nodes
Prediction of early responses to chemotherapy and radiation therapy	Not possible with qualitative evaluation alone
Evaluation of treatment responses and the detection of recurrent disease	Differentiation of residual or recurrent neoplastic tissue from posttreatment induced fibrosis or necrosis is often challenging

CRC: Colorectal cancer.

promotes an irregular architectural vascular pattern<sup>[23]</sup> with areas of low vascular density and regions of high angiogenic activity. Consequently, neoangiogenesis causes structural heterogeneity due to the coexistence of areas of high cell density, necrosis, hemorrhage and myxoid changes within tumoral tissue<sup>[24]</sup>.

The above-described phenomena can be investigated using a functional modality such as PI based on dynamic contrast enhanced (DCE). DCE imaging consists of the acquisition of baseline images before intravenous contrast agent injection, followed by subsequent image acquisition over time<sup>[25]</sup>. PI is an advanced DCE quantitative technique based on the repeated high frequency acquisition of images, which allows the assessment of changes in signal intensity over time. It can be performed with both CT and MRI scanners. PI allows the assessment of vascularity in biological tissues in terms of tumor vessel features (perfusion, permeability, and density), extracellular-extravascular space composition and plasma volume<sup>[25]</sup>. In the following text, we will use the terms DCE and PI interchangeably. A broad spectrum of quantitative parameters can be obtained using PI to assess the vascular properties of pathological tissues<sup>[22]</sup> (Figure 2). A summary of the main PI quantitative parameters used in the assessment of CRC is shown in Table 2<sup>[26,27]</sup>. There is a growing interest in the role of PI in clinical practice for tumor detection and characterization and the assessment of responses to therapy (especially with respect to antiangiogenic treatment strategies) and prognosis.

**Hybrid Imaging:** 18FDG-PET/CT and 18FDG-PET/MRI are molecular and morphological imaging techniques that couple the metabolic and anatomical assessment of tumor lesions<sup>[28]</sup>. 18F-FDG is an analog of glucose that is transported into cells through membrane glucose transporter proteins after intravenous administration<sup>[29]</sup>. Since malignant cells have increased glucose consumption (Figure 3), a preferential accumulation of 18F-FDG occurs in cancer cells compared to normal cells<sup>[30]</sup>. The uptake of 18F-FDG detected by PET can be quantified using parameters such as the standardized maximum or mean uptake value (SUV<sub>max</sub> or SUV<sub>mean</sub>), the metabolic tumor volume (MTV) or the total lesion glycolysis (TLG). The SUV<sub>max</sub> is defined as the uptake value of the pixel with the highest activity inside an ROI divided by the injected dose (which has to be corrected for decay and normalized for the patient's weight or body surface). The SUV<sub>mean</sub> is the average of all the uptake values of the pixels within an ROI. The MTV is defined as the volume of tumor tissues with pathological FDG uptake and calculated as follows: All the voxels inside a tridimensional ROI with SUV values above a determined threshold are included in the final volume; the threshold may be represented by the absolute value ( $\geq 2.5$  or  $\geq 3$  or  $\geq 3.5$ ) or the percentage ( $\geq 20\%$  or  $\geq 30\%$  or  $\geq 40\%$  or  $\geq 50\%$ ) of the SUV<sub>max</sub>. As a result, the MTV incorporates the characteristics of both the volumetric data and the metabolic activity of the tumor. Finally, the TLG is calculated according to the following formula: SUV<sub>mean</sub> × MTV. 18FDG-PET/CT has played a role in clinical practice in the detection of extrahepatic distant metastasis, the evaluation of tumor responses to therapy and the follow-up of treated patients with rising serum carcinoembryonic antigen levels without detectable disease according to morphological imaging.

While the potential use of non-FDG PET radiotracers in CRC imaging is a current topic of investigation, we refrained from discussing this matter in the present review due to the dearth of clinically oriented evidence available in the current literature.

### **Primary tumor identification, tumor grading and differentiation, and local staging**

While endoscopy is considered the main diagnostic tool for the detection of CRC,

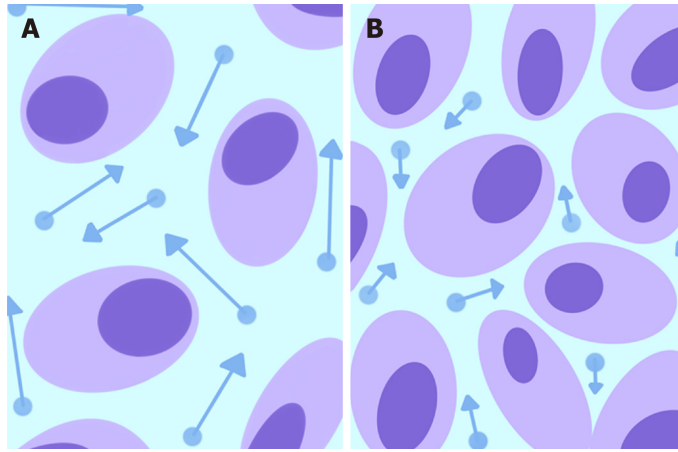


**Figure 1** Schematic representation of water molecule diffusion (dots) in the extracellular space. Normal tissues (A) show a relatively larger extracellular space with high water diffusion (longer arrow vectors higher ADC values), whereas the increased tissue cellularity in a neoplasm (B) reduces the intercellular space and consequently restricts diffusion (shorter arrow vectors lower ADC values).

imaging has the potential to identify primary tumors. Nevertheless, both malignant and benign abnormalities (*e.g.*, inflammatory bowel disease, complicated diverticulitis, and hyperplastic polyps and adenomas) can present with an increase in bowel wall thickness or as polypoid lesions. When using conventional imaging, differential diagnosis is mainly based on morphological features (*e.g.*, lesion size and longitudinal extension, the evaluation of the transitional zone between pathological and healthy mucosa, the presence of focal or multifocal intestinal involvement, the preservation of mural stratification, and the pattern of mesenteric and lymph node involvement). Although all these characteristics contribute the most to the determination of the correct diagnosis, parametric imaging could increase the overall diagnostic accuracy; moreover, it may be useful for the tumor grading and differentiation and local staging.

**DWI with ADC maps:** ADC values have been investigated as possible quantitative parameters that are useful for differential diagnosis. Kilickesmez *et al.*<sup>[31]</sup> reported that mean ADC values may be used to differentiate recto-sigmoid malignancy from both normal rectum and inflammatory bowel disease-affected tissues. The mean ADC value ( $0.97 \times 10^{-3} \text{ mm}^2/\text{s}$ ) of the recto-sigmoid tumor group was significantly different from those of the healthy control ( $1.47 \times 10^{-3} \text{ mm}^2/\text{s}$ ) and inflammatory bowel disease groups ( $1.37 \times 10^{-3} \text{ mm}^2/\text{s}$ ). A recent meta-analysis<sup>[32]</sup> reported that the ADC values of CRC malignant lesions ranged from  $0.97 \times 10^{-3} \text{ mm}^2/\text{s}$  to  $1.19 \times 10^{-3} \text{ mm}^2/\text{s}$ , while those of benign lesions ranged from  $1.37 \times 10^{-3} \text{ mm}^2/\text{s}$  to  $2.69 \times 10^{-3} \text{ mm}^2/\text{s}$ .

The ADC value might serve as a potential noninvasive biomarker of CRC tumor aggressiveness. Indeed, Curvo-Semedo *et al.*<sup>[33]</sup> reported significantly lower ADC mean values in poorly differentiated versus well-differentiated RC, as well as in a T3-T4 stage group versus a T1-T2 stage group. Additionally, Tong *et al.*<sup>[34]</sup> showed a negative correlation between ADC values and extramural maximal depth in RC.

**PI:** Quantitative perfusion parameters have been reported as feasible tools that could be used to discriminate between CRC and noncancerous diseases. Goh *et al.*<sup>[35]</sup> reported that the blood volume (BV), blood flow (BF), mean transit time (MTT), and permeability-surface area product (PS) determined based on perfusion CT were significantly different between patients with CRC and diverticulitis. In particular, the CRC group showed significantly higher BV, BF and PS and a shorter MTT compared to the diverticulitis group. These findings are correlated with neoangiogenesis processes associated with CRC growth. Similarly, Shen *et al.*<sup>[36]</sup> showed that transfer constant (Ktrans) values obtained from perfusion MRI were significantly higher in rectal cancer (RC) compared to those in benign abnormalities ( $0.267 \text{ min}^{-1} \pm 0.07$  vs  $0.118 \text{ min}^{-1} \pm 0.03$ ), indicating that significant angiogenesis and abnormal vasculature enhanced the influx of the contrast agent. Using a  $0.156 \text{ min}^{-1}$  cut-off value for Ktrans, a sensitivity of 100.0% and a specificity of 93.3% were observed when discriminating RC patients from controls.

Sun *et al.*<sup>[37]</sup> reported that the mean BF and BV obtained from perfusion CT were significantly different among well, moderately, and poorly differentiated tumors ( $61.17 \pm 17.97$ ,  $34.8 \pm 13.06$  and  $22.24 \pm 9.31 \text{ mL/min/100 g}$ , respectively). The same

**Table 2** Main quantitative parameters extracted from perfusion imaging of colorectal cancer

Parameter name	Parameter definition	Parameter significance
Regional blood flow	Blood flow per unit volume or mass of tissue, expressed in mL of blood/min/100 mL tissue	It reflects the rate of the delivery of oxygen and nutrients to a certain tissue
Regional blood volume	Volume of capillary blood contained in a certain volume of tissue, expressed in mL blood/100 mL of tissue	It reflects the functional vascular volume
Mean transit time	Mean time needed for blood to pass through the capillary network, expressed in seconds	It reflects the time required for the contrast agent bolus to pass through tissue
Permeability-surface area product (PS)	Flow of molecules through the capillary membranes in a certain volume of tissue, expressed in mL/min/100 mL tissue	It reflects the vascular leakage rate in the microcirculation
Transfer constant (KTrans)	Rate at which the contrast agent transfers from the blood to the interstitium (rate of contrast extraction)	It reflects the balance between capillary permeability and blood flow in a tissue
Tissue interstitial volume (Ve)	Volume of extravascular and extracellular contrast agent in a certain tissue, expressed as a percentage	It is a measure of cell density
Rate constant (Kep)	Rate at which the contrast agent returns from the extravascular-extracellular space to the vascular compartment: $Kep = Ktrans/Ve$	It reflects the tissue microcirculation and contrast agent permeability

working group confirmed these findings, providing further evidence that BF, when determined using perfusion CT images, is associated with tumor grade<sup>[38]</sup>.

**Hybrid imaging:** Due to its utilization of a combination of morphological and molecular information, 18FDG-PET/CT has a high sensitivity for the detection of colorectal lesions. However, unlike determinations based on metabolic information, there is no established consensus regarding the discrimination of benign lesions from premalignant or malignant lesions based on visual appearance alone. A quantitative approach to focal colorectal uptake has been investigated. A few studies have observed that PET quantitative parameters could help to differentiate benign from premalignant or malignant lesions<sup>[39]</sup>, while there have been other studies that have found the opposite<sup>[40,41]</sup>. Moreover, a quantitative approach may be useful for local staging. Liao *et al*<sup>[42]</sup> reported that quantitative parameters such as MTV calculated with a 2.5 threshold aided in discriminating the pT1-T2 group from the pT3-T4 group in patients with RC. The MTV2.5 values for the pT1-T2 and pT3-T4 patient groups were  $11.6 \pm 11.4$  and  $34.6 \pm 21.4$ , respectively. Using the median value of 28 mL as a cut-off, MTV2.5 provided excellent specificity (92.8%) and a positive predictive value (97.1%) for the T3-T4 group, helping to identify patients who would benefit from preoperative chemoradiation therapy (CRT).

#### **Lymph node involvement**

Nodal involvement has an important role in the stratification of risk for CRC patients, and an accurate assessment of this parameter could significantly influence therapeutic management and prognosis. Morphological criteria (size, margins, structural disomogeneity, and clustering) have been used for the detection of pathological lymph node involvement<sup>[43-47]</sup>; however, this approach is still highly debated.

**DWI with ADC maps:** Quantitative ADC values extracted from DWI have been proposed as tools to differentiate between benign and malignant lymph nodes; however, their role remains unclear in this setting. Heijnen *et al*<sup>[48]</sup> reported that DWI can facilitate lymph node detection during the primary staging of RC, but although the ADCmean value was higher for benign nodes compared to malignant nodes ( $1.15 \times 10^{-3} \text{ mm}^2/\text{s}$  vs  $1.04 \times 10^{-3} \text{ mm}^2/\text{s}$ ), the difference was not statistically significant. Lambregts *et al*<sup>[49]</sup> assessed the performance of ADC measurements for nodal restaging in patients with RC undergoing preoperative CRT. The authors reported that the ADCmean value of malignant lymph nodes after CRT was significantly higher compared to that of benign lymph nodes ( $1.43 \times 10^{-3} \text{ mm}^2/\text{s} \pm 0.38$  vs  $1.19 \times 10^{-3} \text{ mm}^2/\text{s} \pm 0.27$ )<sup>[49]</sup>. This finding was attributed to the induction of posttreatment necrosis, which increases the diffusivity and consequently the ADC value. However, the overlapping of ADC values between benign and malignant nodes resulted in insufficient accuracy when ADC values were used alone for the detection of nodal metastases after CRT.

**PI:** PA of PI could further increase the diagnostic accuracy of conventional imaging

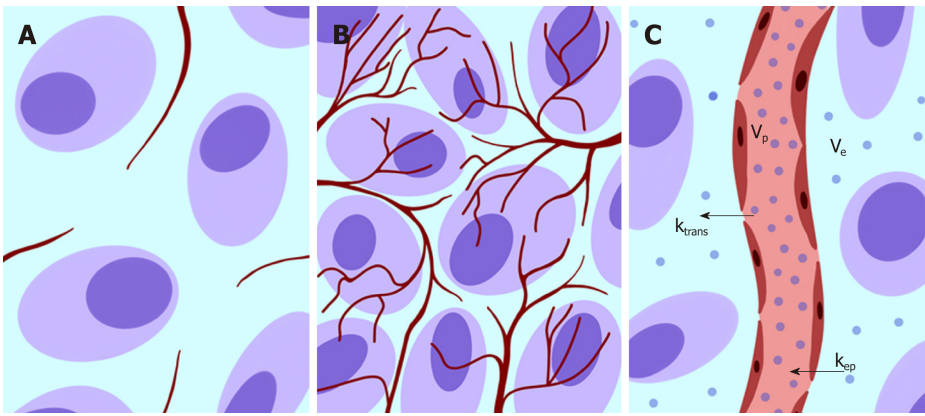


**Figure 2** Schematic representation showing vascularization changes in normal tissue (A) and neoplastic neoangiogenesis (B). In C, a typical bicompartamental model (extended Toft's model) is depicted with various parameters that can be assessed according to the tissue contrast agent concentration (dots) and the arterial input function data.

for nodal involvement evaluation in RC patients<sup>[50-54]</sup>. Ambruster *et al*<sup>[50]</sup> have reported that DCE-MRI quantitative maps increase both the sensitivity (86% *vs* 71%) and specificity (90% *vs* 70%) of conventional MRI for the detection of malignant lymph nodes in locally advanced RC (LARC). Grovik *et al*<sup>[51]</sup> and Yeo *et al*<sup>[52]</sup> found that  $K_{trans}$  values obtained for primary tumors with perfusion MRI were strongly correlated with nodal status in surgical specimens. Yu *et al*<sup>[55]</sup> reported that metastatic lymph nodes from RC showed significantly higher  $K_{trans}$  values and tissue interstitial volume ( $V_e$ ) compared with nonmetastatic lymph nodes during perfusion MRI of lymph nodes with short axis diameters > 5 mm ( $K_{trans}$ :  $0.484 \text{ min}^{-1} \pm 0.198$  *vs*  $0.218 \text{ min}^{-1} \pm 0.116$ ;  $V_e$ :  $0.399 \pm 0.118$  *vs*  $0.203 \pm 0.096$ ). Conversely, Yang *et al*<sup>[54]</sup> demonstrated that the  $K_{trans}$  values were significantly lower in metastatic lymph nodes from RC during perfusion MRI of lymph nodes with short axis diameters < 5 mm. However, when using a  $K_{trans}$  cut-off value of  $0.088 \text{ min}^{-1}$  to differentiate between positive and negative lymph nodes, a sensitivity of 60.5% and a specificity of 81.5% were observed.

**Hybrid imaging:** Qualitative evaluation with 18FDG-PET/CT for the assessment of nodal involvement has limited advantages compared to evaluation with CT<sup>[56,57]</sup>, but a quantitative approach might be utilized to overcome this limitation. Tsunoda *et al*<sup>[58]</sup> compared the diagnostic accuracy of visual analysis and SUVmax evaluation for lymph node metastases using 18FDG-PET/CT in patients with CRC. The sensitivity, specificity and accuracy were 28.6%, 92.9% and 75.0%, respectively, when using a visual approach, while they were 53.1%, 90.6% and 80.1%, respectively, when using a SUVmax cut-off value of 1.5. The mean SUVmax of the malignant lymph nodes (6.3; range: 1.0-33.8) was significantly higher than that of the benign lymph nodes (2.5; range: 1.3-3.3). Similarly, Yu *et al*<sup>[59]</sup> observed that a quantitative approach based on the use of SUVmax might improve the detection of regional lymph node metastasis when using 18FDG-PET/CT in patients with CRC. A significant difference in SUVmax between metastatic and benign juxtaintestinal lymph nodes was observed. When using a cut-off value for SUVmax of 2.0, the corresponding sensitivity, specificity, PPV and NPV were 91.4%, 87.8%, 69.6% and 97.1%, respectively.

### **Response to treatment: efficacy prediction and the assessment of neoadjuvant CRT in RC**

CRT has become the standard of care for LARC. This treatment is associated with fewer local recurrences and may also result in improved long-term survival. The preoperative noninvasive assessment of CRT response in LARC is crucial for planning the surgical approach. MRI is largely used for the local restaging of LARC after neoadjuvant CRT; however, conventional morphological sequences have intrinsic limitations when used for the differentiation of residual viable tumors from surrounding fibrosis<sup>[60,61]</sup>. The overall accuracy of local neoplastic restaging using only morphological T2-weighted (T2w) sequences after CRT is reported to be 47-52%<sup>[61,62]</sup>. CRT induces the necrosis of neoplastic tissue as well as reductions in cellular density and metabolism, increases in the extracellular space and the suppression of neoangiogenesis (Figure 4); these phenomena can be investigated *via* PA of tomographic images.

**DWI with ADC maps:** Several studies<sup>[49,63-65]</sup> have shown the usefulness of ADC values for the assessment of tumor responses to preoperative CRT, suggesting that the

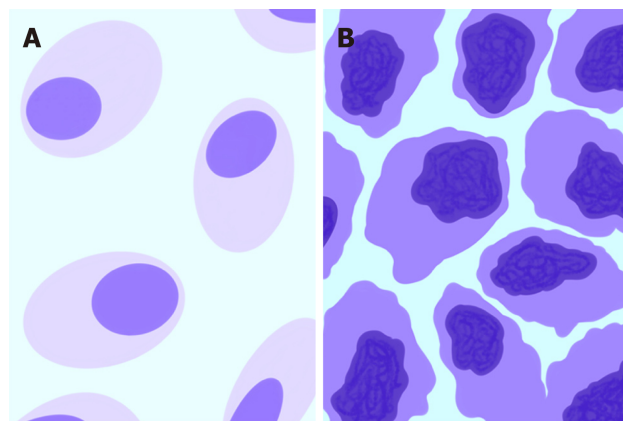


**Figure 3** Schematic representation of morphological and metabolic features of normal tissue (A) compared with those of neoplastic malignant cells (B). The darker shade of violet represents the higher glucose consumption typical of malignant cells.

increase of ADC values after CRT is associated with a good response to preoperative CRT. The absence of ADC value changes during CRT could be used to identify nonresponding patients<sup>[66]</sup>. The increase in ADC in neoadjuvant CRT responders may be due to cell death, cellular membrane disruption and decreased cellularity, which contribute to increased water diffusion. Regarding the assessment of post-CRT residual tumors in LARC, Song *et al*<sup>[67]</sup> reported that the mean ADC after CRT of viable tumors ( $0.93 \times 10^{-3} \text{ mm}^2/\text{s}$ ) differed significantly from that of nonviable tumors ( $1.55 \times 10^{-3} \text{ mm}^2/\text{s}$ ). Moreover, when an ADC value of  $1.045 \times 10^{-3} \text{ mm}^2/\text{s}$  was used as a cut-off value for distinguishing between viable and nonviable tumors, false positive findings were not observed, resulting in a specificity and positive predictive value of 100%. In the same clinical setting, Grosu *et al*<sup>[68]</sup> reported that the ADCmean after CRT of viable tumors ( $1.02 \times 10^{-3} \text{ mm}^2/\text{s}$ ) differed significantly from that of scar tissue ( $1.77 \times 10^{-3} \text{ mm}^2/\text{s}$ ). An ADC cut-off value of  $1.34 \times 10^{-3} \text{ mm}^2/\text{s}$  resulted in a sensitivity, specificity, and accuracy of 93%, 91%, and 92%, respectively. Bassaneze *et al*<sup>[69]</sup> reported that patients with pathological complete responses (pCRs) to neoadjuvant treatment differed significantly from those with non-pCRs in terms of the absolute value of the post-CRT ADC. The mean post-CRT ADC value was  $1.53 \times 10^{-3} \text{ mm}^2/\text{s}$  in the pCR patient group and  $1.16 \times 10^{-3} \text{ mm}^2/\text{s}$  in the non-pCR patient group. All patients with residual tumors in the surgical specimen showed ADC values that were below the cut-off of  $1.49 \times 10^{-3} \text{ mm}^2/\text{s}$ .

However, conflicting results have been reported regarding the value of pretreatment tumor ADC values for the prediction of CRT response in patients with LARC when using surgical specimens as the standard of reference. Some authors observed significantly lower pretreatment ADC values in good responders compared to nonresponders<sup>[70,71]</sup>. Conversely, others reported that the pretreatment ADC values were not significantly different between responders and nonresponders<sup>[72]</sup>.

**PI:** Perfusion CT quantitative parameters have been evaluated for the prediction and assessment of the response of LARC to neoadjuvant CRT. Bellomi *et al*<sup>[73]</sup> reported that the baseline BF and BV were significantly higher and the MTT was significantly lower in responders compared to nonresponders. Conversely, Sahani *et al*<sup>[74]</sup> and Curvo-Semedo *et al*<sup>[75]</sup> reported that the baseline BF was significantly higher and the MTT was significantly lower in non-responders compared to responders. Additionally, both groups<sup>[73,75]</sup> reported a reduction in BF, BV and PS and an increase in MTT after CRT. These perfusion changes are thought to be due to CRT-related fibrosis, which causes the compression of tumor capillaries, a decreased number of arteriovenous shunts, an increased resistance to flow and a reduced volume in the vascular bed<sup>[76]</sup>. A reduction of 40% or more in BF, BV and permeability was observed in patients with RC who responded to neoadjuvant therapy<sup>[22,77]</sup>.

A few studies have evaluated the usefulness of perfusion MRI quantitative parameters for predicting and assessing responses to preoperative treatment in LARC. Lim *et al*<sup>[78]</sup> reported that pre-CRT Ktrans values were significantly higher in the downstaged group after CRT than in the non-downstaged group. Tong *et al*<sup>[79]</sup> reported that patients with pCR had significantly higher Ktrans, Ve and rate constant (Kep) values before CRT than non-pCR patients. In particular, a Ktrans threshold of 0.66 had a sensitivity of 100% for predicting pCR. Gollub *et al*<sup>[80]</sup> observed that Ktrans was significantly lower for tumors from patients with pCR compared with patients



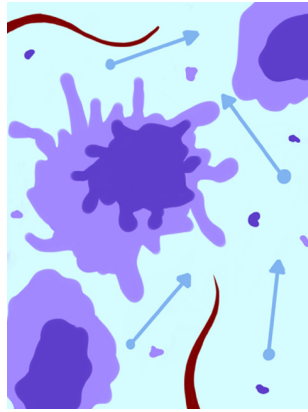


**Figure 4 Schematic representation of neoplastic tissue after treatment.** Cytolysis increases the extracellular space and consequently water diffusion and reduces lesion vascularization and metabolism.

with non-pCR after neoadjuvant chemotherapy; moreover, the posttreatment Ktrans value was correlated with the percentage tumor response and final tumor size according to histopathology. Kim *et al*<sup>[64]</sup> showed a significant reduction in the Ktrans values in the downstaged group after CRT compared to that in the nondownstaged group. Furthermore, the percentage difference between the pre- and post-CRT Ktrans values in the downstaged group was significantly higher compared to that in the nondownstaged group, suggesting that a large decrease in the Ktrans value after CRT was associated with a good response to CRT. DeVries *et al*<sup>[72]</sup> investigated the prognostic value of the perfusion index, which is a microcirculatory perfusion MRI parameter representative of both flow and permeability. The perfusion index was significantly increased in patients who failed to respond to CRT.

A final remark should be made regarding the role of PI in the evaluation of the response to antiangiogenic agents. Bevacizumab is an antiangiogenic monoclonal antibody that targets vascular endothelial growth factor (VEGF). This kind of therapeutic agent often suppresses tumor growth in the absence of notable morphological changes and requires a direct "*in vivo*" evaluation of vascularity to reveal therapeutic results. Willett *et al*<sup>[81]</sup> showed a reduction in BF, BV and PS *via* perfusion CT 12 days after beginning treatment with bevacizumab alone in LARC patients.

In summary, high baseline values and marked post-CRT decreases in perfusion parameters (BF, BV and Ktrans) are predominantly reported in patients with good response. This observation suggests that highly perfused tumors may provide better access for chemotherapy, better oxygenation and higher radiosensitivity compared with poorly perfused tumors. Conversely, the following two neoplastic features may explain a high baseline perfusion parameter in patients who fail to respond to neoadjuvant CRT: (1) The presence of arteriovenous shunts, which is accompanied by a high perfusion rate but a low exchange of nutrients/chemotherapy; and (2) Tissue hypoxia, which induces a high perfusion rate.

**Hybrid imaging:** Several studies have investigated the role of 18FDG-PET/CT in the evaluation of responses to CRT in LARC patients. Lambrecht *et al*<sup>[70]</sup> observed that changes in SUVmax during (after 10-12 fractions) and 5 wk after CRT with respect to the SUVmax value prior to the beginning of CRT ( $\Delta$ SUVmax) were significantly correlated with the pathological response to treatment. Janssen *et al*<sup>[82]</sup> reported that a cut-off value representing a 48% reduction in SUVmax after 2 wk of CRT in patients with LARC resulted in a specificity of 100% and a sensitivity of 64% when differentiating pathological responders from nonresponders. Maffione *et al*<sup>[83]</sup> performed a systemic review of the early prediction of responses by 18FDG-PET/CT during neoadjuvant CRT in LARC. The percentage decrease in SUVmax showed a high accuracy (mean sensitivity 82%; pooled sensitivity 85%) in terms of the early prediction response when using a mean cut-off of 42%. As a result, the early assessment of nonresponding patients allows the modification of the treatment strategy, especially in terms of timing and the type of surgical approach used. It should be noted that radiation-induced inflammation could cause increased 18FDG uptake, possibly reducing PET specificity<sup>[82,84-87]</sup>. To overcome this limitation, the use of dual-time 18F-FDG PET has been proposed. This requires two PET scans; the first is conducted 40-60 min after the injection of 18F-FDG (standard time), and the second is conducted 90-270 min after injection (delayed time), thus allowing the evaluation of

18FDG uptake over time. While 18FDG uptake due to inflammation appears to be stable or to decrease over time, neoplastic 18FDG uptake tends to increase<sup>[88]</sup>. Yoon *et al*<sup>[89]</sup> compared the accuracy of pre-CRT standard and post-CRT dual-time 18FDG-PET/CT in the prediction of CRT responses in LARC patients. The quantitative dual-time score (defined as the delay index [DI], which is equal to post-SUVmax-early - post-SUVmax-delayed/post-SUVmax-delayed of post-CRT 18FDG-PET/CT) showed significantly better performance with a higher area under the curve value (0.906 *vs* 0.696,  $P = 0.018$ ) than the standard quantitative score (defined as the response index [RI], which is equal to pre-SUVmax - post-SUVmax/ pre-SUVmax). The DI showed a sensitivity of 86.7%, a specificity of 87%, a PPV of 68.4% and a PNV of 95.2%, suggesting that dual-time post-CRT PET/CT might be the most appropriate diagnostic tool for this specific setting.

### **Responses to treatment: colorectal liver metastases**

Surgical resection remains the only treatment with curative potential for colorectal liver metastases (CRLMs)<sup>[89]</sup>. In patients who are not suitable candidates for surgery, chemotherapy alone or in combination with local hepatic treatments, such as intrahepatic arterial infusion chemotherapy, transcatheter arterial chemoembolization (TACE), selective internal radiation therapy (SIRT), radiofrequency ablation (RFA), laser therapy or cryotherapy, may be performed<sup>[90]</sup>. Tomographic imaging based on conventional qualitative evaluation contributes mostly to defining the appropriate therapeutic management of CRLMs<sup>[91,92]</sup>; however, defining tumor biology could allow the improved selection of treatment strategies and, as a result, the more accurate prognostic evaluation of patients<sup>[90]</sup>. In this setting, PA could provide potentially useful imaging markers for the prediction of treatment response.

**DWI with ADC maps:** ADC values have been proposed for use in assessing the responses of CRLMs to chemotherapy<sup>[93,94]</sup>. Koh *et al*<sup>[93]</sup> reported that high mean pretreatment ADC values for CRLMs were associated with poorer responses to chemotherapy (nonresponder:  $1.55 \times 10^{-3} \text{ mm}^2/\text{s}$ ; responder  $1.36 \times 10^{-3} \text{ mm}^2/\text{s}$ ). Indeed, high ADC values are observed in necrotic areas, which typically show poor perfusion and allow only limited local delivery of chemotherapeutic drugs. Cui *et al*<sup>[94]</sup> found that CRLMs showed significantly decreased mean pretreatment ADC values in responding lesions ( $0.95 \times 10^{-3} \text{ mm}^2/\text{s} \pm 0.15$ ) than in nonresponding lesions ( $1.18 \times 10^{-3} \text{ mm}^2/\text{s} \pm 0.27$ ). Furthermore, an early increase in ADC values was observed in responding lesions after 3 or 7 d of treatment.

**PI:** Few studies have been performed to assess the utility of quantitative PI parameters as biomarkers for the assessment of CRLM responses to treatment. Using baseline perfusion MRI and follow-up MRI evaluated on the basis of RECIST 1.1 criteria in patients with CRLMs treated with a combination of chemotherapy and bevacizumab, Coenegrachts *et al*<sup>[95]</sup> found significantly higher Kep values in responders than in nonresponders (responders: 0.09852; nonresponders: 0.07829). Moreover, the Kep values were significantly decreased in responding patients compared to nonresponding patients after 6, 12 and 18 weeks of treatment, suggesting that Kep values may be able to predict early treatment response in CLRMs.

**Hybrid imaging:** Few studies have investigated the possible role of quantitative parameters derived from 18FDG-PET/CT in the assessment of CLRM treatment responses. Recently, Nishioka *et al*<sup>[96]</sup> observed that an SUVmean value cut-off of 3 and morphological CT criteria<sup>[10]</sup> had similar excellent predictive power for  $\leq 10\%$  tumor viability (areas under the curve of 0.916 and 0.882, respectively) compared to that for the degree of tumor shrinkage (area under the curve of 0.69) in patients who underwent PET/CT after chemotherapy and before the surgical resection of CRLMs.

### **CRC prognosis**

Tumor stage at diagnosis is considered the most important prognostic factor for CRC patients<sup>[97]</sup>. However, other prognostic factors that include biological and molecular information should be taken into account to personalize prognosis<sup>[98]</sup>. Parameters such as tumor differentiation grade and the presence of lymphovascular invasion (LVI)<sup>[99]</sup> are valuable in the prognostic evaluation of RC patients. Similarly, the plasmatic levels of carcinoembryonic antigen (CEA)<sup>[100]</sup> are useful for the prognostic assessment of CRLMs.

As a result, detailed information regarding the individual tumor profile of each patient is critical to determine the risk for local and distant recurrence<sup>[101]</sup>. Measures such as overall survival (OS), progression-free survival (PFS) or recurrence-free survival (RFS) are commonly used for prognostic evaluation. PA has the potential to introduce novel useful biomarkers that could correlate to the biological and genetic prognostic features of CRC and CRLMs or predict OS, PFS and/or RFS.

Consequently, such parameters could be useful in CRC risk stratification and in treatment planning.

**DWI with ADC maps:** The quantitative evaluation of ADC maps derived from DWI could aid in the prediction of patient prognosis<sup>[16,18,70]</sup>. Curvo-Semedo *et al.*<sup>[33]</sup> reported that ADC values differed significantly between RC tumors with and without mesorectal fascia (MRF) invasion, between N0 and N+ cancers and even among different histological grades. In particular, decreased mean pretreatment ADC values were observed in tumors with MRF involvement, metastatic lymph nodes or poorly differentiated grading. Sun *et al.*<sup>[102]</sup> reported that decreased ADC values were strongly associated with increased T stage and a more aggressive tumor profile. Tong *et al.*<sup>[34]</sup> observed that the extramural maximal depth and the ADC value have a significant negative correlation in the T3 RC spread. Heijmen *et al.*<sup>[103]</sup> reported that low prechemotherapy ADC values in CRLMs predicted poorer outcomes in terms of both PFS and OS.

**PI:** Goh *et al.*<sup>[104]</sup> reported that CRC with low BF at staging according to perfusion CT showed an increased tendency to metastasize and resulted in significantly decreased OS. Particularly, a group of patients who had developed metastatic disease prior to follow up presented a mean baseline BF value of 45.7, while the mean BF value of the disease-free group was 76 mL/min/100 g. Similarly, Hayano *et al.*<sup>[76]</sup> reported that patients with RC with increased BF according to perfusion CT survived significantly longer than those with decreased BF. More recently, two studies reported that Ktrans measured *via* DCE-MRI is correlated with the pathological differentiation of RC; poorly differentiated tumors showed increased Ktrans values<sup>[36,105]</sup>. Moreover, Ktrans values were significantly higher in lesions with distant metastasis than in lesions without distant metastasis and in the pLVI positive group than in the pLVI negative<sup>[105]</sup> group.

Finally, perfusion MRI studies conducted on patients with CRLMs treated with bevacizumab are worth mentioning<sup>[106-108]</sup>. Indeed, Hirashima *et al.*<sup>[106]</sup> observed a significant correlation between a reduction in the Ktrans value 7 days after the start of treatment and a longer time to progression. Subsequently, Kim *et al.*<sup>[107]</sup> confirmed this finding and found that a reduction of 40% in the Ktrans cut-off value could be used to discriminate responders from nonresponders. De Bruyne *et al.*<sup>[108]</sup> found that a decrease in Ktrans of more than 40% after bevacizumab chemotherapy in patients with CRLMs was associated with improved PFS.

**Hybrid imaging:** Avallone *et al.*<sup>[109]</sup> evaluated the prognostic role of early metabolic responses to CRT in patients with LARC. In their study, 18FDG-PET scans were performed before and 12 days after the beginning of CRT. Responders, defined on the basis of a reduction in the SUV mean value  $\geq 52\%$  compared to the baseline, showed a 5-year RFS that was significantly higher than that of nonresponders.

Muralidharan *et al.*<sup>[110]</sup> reported that high MTV and TLG values for CRLMs before surgical resection were significantly associated with poorer recurrence-free survival (RFS) and OS, while the SUVmax and SUVmean did not show any significant predictive ability. Lastoria *et al.*<sup>[111]</sup> performed a 18FDG-PET/CT evaluation before and after 1 cycle of FOLFIRI plus bevacizumab treatment in patients with resectable CRLMs. Pathological responses were assessed in patients undergoing resection. For each lesion, a  $\leq -50\%$  change in the SUVmax and the TLG compared to baseline was used as a threshold to indicate a significant metabolic response. An early metabolic PET/CT response had a stronger and more independent and statistically significant predictive value for PFS and OS compared to both CT/RECIST and pathological response according to multivariate analysis. Similarly, Lau *et al.*<sup>[112]</sup> investigated the prognostic value of 18FDG-PET/CT before and after preoperative chemotherapy in patients undergoing the liver resection of CRLMs. SUVmax, MTV, and TGV, their changes (DSUVmax, DMTV, DTGV) and their correlation with RFS and OS were evaluated. DSUVmax was the only parameter predictive of RFS and OS according to multivariate analysis. Patients with metabolically responsive tumors had an OS of 86% at 3 years vs 38% for patients with nonresponding lesions. Gulec *et al.*<sup>[113]</sup> investigated the relationship between MTV and TLG and clinical outcomes in patients with unresectable CRLMs undergoing treatment with 90Y resin microspheres. The authors observed that MTV values below 200 cc during pretreatment PET/TC and below 30 cc during posttreatment PET/CT at 4 wk were significantly associated with a longer median survival compared to MTV values above 200 during the pretreatment exam and 30 cc during the posttreatment exam at 4 wk. Similar results were found for TLG values below and above 600 g during the pretreatment exam and below and above 100 g during the posttreatment exam, respectively.

Giacomobono *et al.*<sup>[114]</sup> evaluated the value of SUVmax for stratifying CRC patients

with unexplained CEA increases and FDG uptake at the site of anastomosis after surgical curative resection. Nonspecific FDG uptake at the anastomotic site was the most frequent cause of error because it could be due to both post-CRT/post-surgical fibrosis/scar tissue and disease recurrence. The anastomotic SUVmax was the only significant predictor of tumor recurrence at the site of anastomosis. A decreased OS was reported in patients with a SUVmax greater than 5.7 compared with that in patients with lower values (median survival: 16 mo *vs* 31 mo;  $P = 0.002$ ). Marcus *et al*<sup>[115]</sup> showed that a decreased MTVtotal and TLGtotal were associated with increased OS in patients with local, loco-regional and/or distant-recurrent biopsy-verified CRC.

## OTHER ADVANCED QUANTITATIVE FUNCTIONAL AND MOLECULAR IMAGING MODALITIES

Blood oxygenation level-dependent (BOLD) MRI and MR spectroscopy (MRSI) represent further advanced imaging modalities available for use with quantitative PA in CRC.

BOLD-MRI is able to assess *in vivo* tissue hypoxia according to blood flow and the paramagnetic properties of deoxyhemoglobin within red blood cells<sup>[116]</sup>. Endogenous deoxyhemoglobin decreases the transverse relaxation rate ( $T2^*$ ) in blood, which can be quantified by  $R2^*$  ( $= 1/T2^*$ )<sup>[117,118]</sup>. Tumor hypoxia is caused by the inability of the neoplastic vascular system to provide an adequate supply of oxygen to the growing tumor mass. Tumor hypoxia induces the expression of the transcription factor hypoxia inducible factor-1 alpha (HIF-1 $\alpha$ ), which promotes the adaptation of cancer cells to hypoxia and the development of more aggressive clones less sensitive to radiotherapy and chemotherapy<sup>[119]</sup> and impacts metastatic spread to favor tumor recurrence and a poor prognosis. Heijmen *et al*<sup>[103]</sup> investigated the ability of BOLD-MRI to predict outcomes and responses to systemic treatment in patients with CRLMs undergoing MRI before and one week after the beginning of first-line chemotherapy. The authors reported that a low pretreatment  $T2^*$  value in CRLMs (indicating a higher concentration of deoxyhemoglobin) was a significant predictor for increased OS; however, the  $T2^*$  value did not significantly change one week after the beginning of treatment, which did not make it a useful predictor of the response to therapy.

MRSI is a noninvasive technique that allows the measurement of metabolites and metabolic processes in normal and pathological tissues<sup>[120]</sup>. The resonance frequencies of the metabolites are expressed in parts per million (ppm). Tumor tissues are characterized by disordered energy metabolism (an increased lactate concentration due to anaerobic glycolysis and the activation of the creatine/phosphocreatine system), amino acid metabolism (the accumulation of amino acids due to the increased turnover of structural proteins) and choline metabolism (increased levels of choline, which is a marker of cellular membrane turnover related to cell proliferation)<sup>[121]</sup>. Dzik-Jurasz *et al*<sup>[122]</sup> demonstrated the presence of choline and lipid peaks in patients with RC. Kim *et al*<sup>[120]</sup> reported that a choline peak at 3.2 ppm in patients with RC disappeared after radiation therapy and chemotherapy.

Both of these modalities suffer from limited clinical applicability due to their high intrinsic technical complexity; furthermore, there are still insufficient evidence in the literature to define their possible role in CRC clinical management.

## QUANTITATIVE IMAGE ANALYSIS METHODS

### Texture analysis

**Physiological aspects and technical features:** As previously stated, tumor heterogeneity is a hallmark of malignancy that is highly related to tumor biology<sup>[124,123]</sup>, and it can be qualitatively and/or quantitatively evaluated by several imaging modalities. TA is a postprocessing imaging technique that allows heterogeneity quantification to evaluate both the distribution and relationships within the information contained in each voxel<sup>[123]</sup>. The content of this information depends on the imaging modality used (Hounsfield units measure density for CT, signal intensity measures tissue relaxation times for MRI, and standard uptake values measure activity for PET). A broad spectrum of quantitative parameters can be extracted from any diagnostic imaging modality, ranging from first-order parameters (defined on the basis of histogram analysis, which does not account for spatial distribution) to more complex higher-order parameters<sup>[124]</sup>. Multiple first-order parameters are available, including the mean gray-level intensity (brightness), uniformity (distribution of the gray level), entropy (a measure of irregularity), skewness (a measure of the asymmetry of the pixel histogram distribution) and kurtosis (the magnitude of the

pixel histogram distribution)<sup>[125]</sup>. The analysis is performed by drawing an ROI in the largest cross-section of the tumor or in tumor subregions and by taking into account the whole tumor volume or delineating the margins in an organ in the absence of a target lesion. Interestingly, TA approaches can also be employed for morphological images (such as unenhanced CT images or T2-weighted MR images), possibly reducing the need for more complex, expensive and time-consuming techniques. Additionally, filtering techniques can be applied to the original images before performing TA to widen the range of available quantitative parameters<sup>[126]</sup>. Encouraging results have been recently published for TA in the field of oncologic imaging<sup>[127,128]</sup>. Regarding CRC, the application of TA to CT, MRI and PET/CT images has been investigated and might be useful in different clinical settings for characterization, staging, prognosis and treatment planning.

**Primary tumor identification:** The accurate differentiation of colorectal nonneoplastic (i.e., hyperplastic polyps) and neoplastic lesions (i.e., adenomas and adenocarcinomas) based on computed tomography colonography (CTC) for mucosal colorectal lesions is mandatory for appropriate patient management<sup>[129]</sup>. The lesion size is correlated with the risk of malignancy, but size alone is not sufficient to discriminate between nonneoplastic and neoplastic lesions for the following reasons: (1) CTC tends to underestimate polyp size<sup>[130]</sup>; and (2) The overlap in the sizes of benign, premalignant and malignant lesions. Moreover, combination of metabolic and morphological information does not seem to increase the accuracy of CTC<sup>[41]</sup>. Therefore, TA might improve the diagnostic performance of CTC by introducing additional criteria for evaluation. Song *et al.*<sup>[131]</sup> evaluated the accuracy of the use of CTC texture features in differentiating colorectal lesions. Intensity, gradient (i.e., the degree of the intensity change) and curvature (i.e., the degree that a geometric object deviates from being flat) were calculated for each colorectal polyp lesion. The results showed that the combination of gradient and curvature features significantly improved the performance of CTC in differentiating hyperplastic polyps from neoplastic lesions. The skewness and entropy values calculated on the basis of ADC maps were significantly lower in patients with stage pT1-2 tumors versus those with stage pT3-4 tumors<sup>[132]</sup>. Kurtosis values obtained on the basis of DWI were significantly higher in high-grade than in low-grade RC<sup>[133]</sup>.

**Lymph node involvement:** The evaluation of the structural heterogeneity of loco-regional lymph nodes by using TA could help predict nodal status in RC to reliably differentiate malignant lymph nodes from benign lymph nodes. In this regard, Cui *et al.*<sup>[134]</sup> reported that the heterogeneity of benign mesorectal nodes calculated by using enhanced CT images was significantly lower than that of malignant nodes when the short-axis diameter was 3–10 mm. However, no difference was observed between benign and malignant lymph nodes less than 3 mm and larger than 10 mm. Liu *et al.*<sup>[132]</sup> reported that entropy values calculated by using ADC maps were significantly higher in pN1-2 than in pN0 RC. Similarly, Zhu *et al.*<sup>[133]</sup> reported significantly higher kurtosis values calculated by using DWI in pN1-2 compared to pN0 RC.

**Response to treatment: Neoadjuvant CRT in RC:** TA of MR images might identify biomarkers able to assess responses to CRT in patients with LARC<sup>[125,132,135-137]</sup>. Using T2 weighted images, De Cecco *et al.*<sup>[135]</sup> found that pre-neoadjuvant CRT kurtosis was significantly decreased in pCR versus partial-responders or nonresponders. Similarly, using T2 weighted images, Shu *et al.*<sup>[136]</sup> found that TA of a combination of pre- and early-treatment features could distinguish between responders and nonresponders. TA approaches based on advanced sequences such as DCE<sup>[137]</sup> and ADC maps<sup>[132]</sup> have also been proposed and have shown promising results.

**CRLMs: early identification and responses to treatment:** Liver colonization by CRC cells is considered to be a multiple step process that progresses from prometastatic hepatic reactions to micrometastases and finally generates macrometastases<sup>[138]</sup>. The liver prometastatic reaction produces a special microenvironment favoring liver colonization by tumor cells. This reaction begins in the early tumor stage with the release of cytokines and chemokines by hepatic sinusoidal endothelium and Kupffer cells in response to colon cancer soluble factors and circulating cells. Cytokines and chemokines lead to the activation of perisinusoidal stellate cells and portal tract fibroblasts, which deposit extracellular matrix and create stromal support for cancer cells. The early preoperative identification of prometastatic hepatic reactions might facilitate the use of personalized treatment strategies that involve the selection of chemotherapy independently according to local staging<sup>[139]</sup>. Similarly, the preoperative identification of micrometastases in addition to visible liver metastases might indicate the use of neoadjuvant chemotherapy in CRC patients who are candidates for liver resection<sup>[140]</sup>. Conventional tomographic imaging is unable to detect liver

prometastatic reactions or occult liver micrometastases. A few studies have tested the ability of TA to detect precocious hepatic alterations on the basis of the fact that the spatial heterogeneity of an apparently disease-free liver may be altered by liver prometastatic reactions and occult liver micrometastases.

Rao *et al*<sup>[140]</sup> assessed the capability of whole-liver portal phase CT TA to detect structural differences between apparently disease-free liver parenchyma in CRC patients without and with liver metastases. Disease-free liver parenchyma in patients with synchronous liver metastases (Group B) showed entropy values significantly higher and uniformity values significantly lower than those in patients without liver metastases (Group A). Furthermore, the disease-free liver parenchyma in patients who developed metachronous liver metastases within 18 months after primary staging CT (Group C) showed a subtle trend towards increased entropy and decreased uniformity values compared to that in patients in group A, although the difference was not significant. These results produced the following observations: (1) Group B presented greater heterogeneity in the liver parenchymal structure compared to group A due to the possible presence of micrometastases in the apparently disease-free remaining liver tissues or tumor-induced changes in liver perfusion; and (2) Group C may show ongoing tumor-induced, structural and/or hemodynamic changes in the liver parenchyma that precede morphological changes, allowing the identification of patients at risk of developing metachronous hepatic metastases.

Finally, both CT- and MRI-based TA parameters have been explored as feasible tools to predict treatment responses in patients with CRLMs<sup>[141,142]</sup>. Zhang *et al*<sup>[141]</sup> evaluated the response to chemotherapy of 193 unresectable liver metastases using dimensional reduction that was observed by the comparison of T2-weighted pretreatment and posttreatment MR images as a reference standard (a cutoff of a 30% decrease in the maximum diameter defined the responders). The authors found that the association of a first-order parameter (variance) and a higher-order parameter (angular second moment) had the ability to predict response, with an AUC of 0.814. Likewise, Ahn *et al*<sup>[142]</sup> demonstrated that decreased skewness values, obtained from two-dimensional ROIs used to annotate liver metastases on CT portal-phase images, were predictive of responses to chemotherapy (AUC = 0.797).

**Prognosis:** Ng *et al*<sup>[143]</sup> showed a correlation between the entire primary CRC heterogeneity according to portal venous CT images with the 5-year OS rate. CRC with decreased heterogeneity (decreased entropy, kurtosis and standard deviation of pixel distribution; increased uniformity and skewness) was associated with a decreased 5-year OS.

Miles *et al*<sup>[144]</sup> assessed the ability of the TA of hepatic portal phase CT images to predict survival in patients with CRC subject to surveillance for at least 24 months after tumor resection. Kaplan-Meier curves showed that increased uniformity was a significant predictor of survival. Finally, Lovinfosse *et al*<sup>[145]</sup> evaluated the TA of baseline 18FDG-PET/CT in LARC patients and concluded that increased coarseness values may be indicative of worse outcomes.

### Volumetry

CT, MRI and PET hybrid imaging allow the “*in vivo*” calculation of neoplastic volume. RC tumor burden is correlated with disease stage and represents an important prognostic feature in terms of the prediction of treatment response, OS and PFS after CRT<sup>[146-149]</sup>. The tumor volume reduction rate has been reported to be superior to RECIST criteria for the prediction of the pathological responses of RC to neoadjuvant CRT<sup>[150]</sup>.

The determination of tumor volumetry by using morphological CT and MR images requires the delineation of the neoplastic contours, which can be defined visually by manually tracing the presumed lesion boundary in each image containing the neoplasm. The volumes of the lesions are calculated by adding each of the 2D volumes (multiplying the 2D area by image thickness) of the entire lesion. The following considerations can explain the limits of this qualitative visual approach for tumor volumetry measurement: (1) Inflammatory peritumoral reactions can hamper the exact delineation of the interface between the tumor and the surrounding tissues; and (2) The difficulty in distinguishing between therapy-induced fibrosis and the residual viable tumor can also be problematic. A quantitative parametric analysis of images has also been proposed to solve this problem of tumor volumetry measurement.

T2-weighted signal intensity-selected volumetry of post-CRT MRI performed better than visual qualitative T2 volumetry in predicting pCR in patients with LARC<sup>[151]</sup>. Posttreatment total lesion diffusion (TLD = total DWI tumor volume × mean volumetric ADC) was better correlated than the total DWI tumor volume with histopathological tumor responses after CRT in patients with LARC<sup>[152]</sup>.

## LIMITATIONS AND POTENTIAL EFFECTIVE CLINICAL APPLICATIONS OF PARAMETRIC IMAGING ANALYSIS

### **DWI with ADC maps**

Well-defined cut-off values are needed to use ADC maps in routine clinical practice. The ADC value thresholds used for differentiating normal and pathological tissue, assessing responses to therapy and defining prognosis have not yet been established for CRC. The lack of definite thresholds may be attributed to the following: (1) ADC values depend on the scanner and the acquisition protocol used and the clinical setting; (2) ADC values are subject to measuring errors due to the low spatial resolution of DWI images; and (3) The lack of reproducibility for ADC measurements. ADC values appear to be particularly promising for the prediction and assessment of RC responses to neoadjuvant CRT.

### **Perfusion imaging**

The following general principles concerning angiogenesis and CRC have been established: More poorly perfused tumors usually lead to a poorer outcome; baseline perfusion is significantly higher in responders than in nonresponders to several types of therapies; and an early reduction in vascular parameters after therapy is usually associated with improved patient outcome<sup>[22]</sup>. The use of PI techniques has not yet been introduced in routine clinical practice, probably due to the numerous different technical approaches required and the complexity of parameter measurement. The following limitations of PI have to be considered: (1) The quantification of contrast agent concentrations is challenging because of the complex relationship between density (CT) or signal (MRI) and the contrast medium concentration, which is dependent on many factors, including the contrast agent dose, rate of injection, time of circulation, machine parameters, and, for MRI, native tissue relaxation rates and imaging sequence; (2) The different models used for the analysis of DCE imaging data and the calculation of quantitative perfusion parameters<sup>[153]</sup> may influence the measurement of quantitative perfusion parameters<sup>[35]</sup>; and (3) Tumor ROI analysis with current DCE imaging software platforms utilizes the mean quantitative vascular parameters, which do not reflect the spatial heterogeneity of perfusion<sup>[154]</sup>. Because of the large variety of potential indicators that could be used as imaging biomarkers, PI still needs further study to be recognized as an effective diagnostic tool in routine clinical practice. Among all the potential clinical applications of DCE imaging for CRC, the assessment and prediction of responses to antiangiogenic agents appears to be the most promising.

### **Hybrid imaging**

<sup>18</sup>F-FDG-PET/CT quantitative parameters have added value for routine clinical practice. The following topics may benefit from a quantitative approach: The improvement of the detection of regional lymph node metastases; the prediction and assessment of RC responses to neoadjuvant CRT; the detection of tumor recurrence after surgery in combination with serum CEA levels. There is not enough scientific evidence to recommend the routine use of quantitative <sup>18</sup>F-FDG-PET/CT for the identification and/or local staging of primary CRC because PET has the following limitations: (1) FDG uptake depends on several features, including tumor grade, the type of tumor involvement, histological type (*e.g.*, FDG is limited in the evaluation of mucinous tumors); and (2) Limited spatial resolution, which may cause small lesions to be missed.

### **Texture analysis**

Texture analysis mainly suffers from the following limitations: (1) The biological correlations of TA measurements have not been established definitively; and (2) The image acquisition parameters (for CT: Tube voltage, tube current, collimation; for MRI: features of the sequences) and TA processing (unfiltered or filtered at a fine, medium or coarse scale; TA calculation of single axial sections or whole target volumes; the use of semiautomated and automated systems to delineate tumor regions or volumes) may affect the measurement of TA parameters and may change their biological correlation. TA represents an ongoing topic of investigation, but the clinical effectiveness of the technique still has to be defined in different clinical settings relevant to CRC.

## THE NEXT STEPS: MULTI-PARAMETRIC IMAGING ASSESSMENT, RADIOMICS AND RADIOGENOMICS, AND MACHINE LEARNING

The complexity of tumor biology cannot be described by a single morphological, functional and/or molecular parameter. An integrated approach utilizing noninvasive *in vivo* imaging techniques can be used to accurately represent neoplastic heterogeneity. A more comprehensive multiparametric assessment of tumor biology can be obtained from a single examination combining morphological, functional and/or molecular information by using hybrid devices such as PET/CT or PET/MRI. A few studies have investigated the relationships between functional and molecular parameters in CRC. An inverse relationship between tumor vascularization (expressed as the K<sub>ep</sub> value) and metabolism (expressed as SUV<sub>max</sub>) was observed in CRLMs<sup>[155]</sup>. CRCs with a low-flow and high-metabolism phenotype were associated with increased levels of hypoxia-inducible factor 1 (HIF-1 $\alpha$ ), suggesting that flow and metabolism mismatch may represent an adaptive angiogenic response to hypoxia<sup>[156]</sup>. Highly perfused RC manifested with higher FDG uptake levels than low-perfusion tumors, suggesting that tumor growth is accompanied by an intense inflammatory reaction rather than the development of necrosis<sup>[157]</sup>. A significant negative correlation between the ADC and SUV values was reported for adenocarcinomas of the rectum, suggesting that the vital cellular burden is associated with increased metabolism<sup>[158,159]</sup>. The decrease in flow and metabolism (expressed as BF  $\times$  SUV<sub>max</sub>) showed high accuracy in the prediction of histopathological responses to radiation therapy and chemotherapy when using a cutoff value of -75% in patients with RC<sup>[159]</sup>. Multiparametric quantitative assessment appears to be a promising strategy for CRC management; however, its role in the different clinical settings associated with CRC must still be defined.

Further prospective investigations are needed to evaluate the clinical effectiveness of multiparametric imaging and to propose its routine clinical use in CRC settings.

Radiomics has recently emerged as a promising tool for discovering new imaging biomarkers by extracting and analyzing numerous quantitative image features representative of tumor heterogeneity and phenotype. Radiomics combines the imaging of quantitative biomarkers with clinical reports and laboratory test values in a statistical model (Figure 5). Similarly, radiogenomics evaluates the relationship between radiomics and gene-expression patterns or transcriptomic and/or proteomic data to generate a statistical model. These advanced computational techniques can be applied to any type of clinical image, such as CT, MRI or hybrid PET images, and they can be used in a variety of clinical settings for diagnosis, the prediction of prognosis, and the evaluation of treatment response<sup>[160,161]</sup>. Although there is still a limited amount of evidence regarding the applications of radiogenomics to CRC, it retains tremendous potential<sup>[162]</sup>. Indeed, studies conducted using images from different modalities (mainly PET/CT) have investigated the relationship between radiomic data and K-ras gene mutations in CRC patients with encouraging results<sup>[163-165]</sup>. The K-ras gene mutation is an independent prognostic factor for survival and a negative predictive marker of tumor responses to drugs that target anti-epidermal growth factor receptors (EGFRs). Shin *et al*<sup>[163]</sup> reported that the frequency of K-ras mutations was higher in polypoid tumors with a larger axial to longitudinal dimension ratio. Using an animal model, Miles *et al*<sup>[166]</sup> reported that the combined multiparametric assessment of 18F-FDG uptake (expressed as SUV<sub>max</sub>), CT texture (expressed as the mean value of tumor pixels with positive values) and perfusion (expressed as BF) has excellent accuracy (90.1%) in the identification of CRCs with K-ras mutations.

The increasing use of quantitative imaging data in clinical practice will require the use of automated and intelligent systems for analyzing a large amount of numerical information. Artificial intelligence and machine learning approaches can be helpful for the evaluation of radiomic and radiogenomic features. Deep learning convolutional neural networks can perform texture analysis and training with large amounts of data to create predictive algorithms.

## CONCLUSION

The interpretation of medical tomographic images can no longer treat images strictly as pictures but instead must use innovative approaches based on numerical analysis. PA allows the extraction and analysis of the large amount of numerical data hidden in tomographic images. This information must be correlated with genetic, histological, clinical, prognostic and/or predictive data. The transition from purely anatomical tomographic imaging to quantitative tomographic imaging can also benefit the



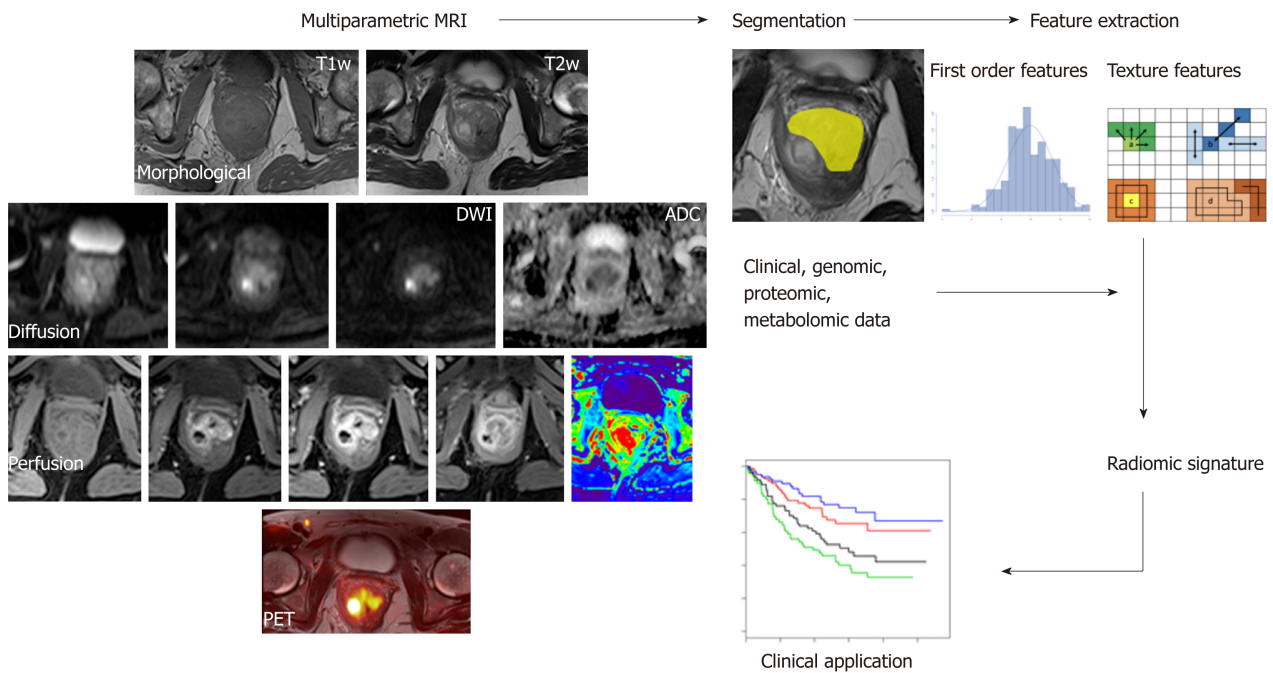


**Figure 5** A typical radiomics workflow consists of several steps. After image acquisition, segmentation is performed to define the tumor region. From this region, several features are extracted based on the intensity histogram and texture analysis. Finally, these features are assessed for their prognostic power or are linked with the stage or gene expression.

diagnostic management of CRC. However, to be of practical value and to have a real effect on clinical CRC diagnostic management, quantitative imaging approaches require the following: (1) The standardization of technical features to ensure the acquisition of good quality data and the development of robust techniques for analysis to assure reproducibility among different operators, scanners and centers; (2) Well-defined cut-off values for each proposed parameter measure in different clinical settings relevant to CRC; (3) A clear definition of the clinical significance of each numerical parameter as a single measure or a multiparametric combination; and (4) A real added-value when used to determine the known clinical and pathological factors of each new numerical imaging biomarker.

## REFERENCES

- 1 Siegel RL, Miller KD, Jemal A. Cancer statistics, 2019. *CA Cancer J Clin* 2019; **69**: 7-34 [PMID: 30620402 DOI: 10.3322/caac.21551]
- 2 Yuan Y, Li MD, Hu HG, Dong CX, Chen JQ, Li XF, Li JJ, Shen H. Prognostic and survival analysis of 837 Chinese colorectal cancer patients. *World J Gastroenterol* 2013; **19**: 2650-2659 [PMID: 23674872 DOI: 10.3748/wjg.v19.i17.2650]
- 3 Labianca R, Nordlinger B, Beretta GD, Mosconi S, Mandalà M, Cervantes A, Arnold D; ESMO Guidelines Working Group. Early colon cancer: ESMO Clinical Practice Guidelines for diagnosis, treatment and follow-up. *Ann Oncol* 2013; **24** Suppl 6: vi64-vi72 [PMID: 24078664 DOI: 10.1093/annonc/mdt354]
- 4 Glynn-Jones R, Wyrwicz L, Tiret E, Brown G, Rödel C, Cervantes A, Arnold D; ESMO Guidelines Committee. Rectal cancer: ESMO Clinical Practice Guidelines for diagnosis, treatment and follow-up. *Ann Oncol* 2018; **29**: iv263 [PMID: 29741565 DOI: 10.1093/annonc/mdy161]
- 5 Van Cutsem E, Cervantes A, Nordlinger B, Arnold D; ESMO Guidelines Working Group. Metastatic colorectal cancer: ESMO Clinical Practice Guidelines for diagnosis, treatment and follow-up. *Ann Oncol* 2014; **25** Suppl 3: iii1-iii9 [PMID: 25190710 DOI: 10.1093/annonc/mdl260]
- 6 Gerlinger M, Rowan AJ, Horswell S, Math M, Larkin J, Endesfelder D, Gronroos E, Martinez P, Matthews N, Stewart A, Tarpey P, Varela I, Phillimore B, Begum S, McDonald NQ, Butler A, Jones D, Raine K, Latimer C, Santos CR, Nohadani M, Eklund AC, Spencer-Dene B, Clark G, Pickering L, Stamp G, Gore M, Szallasi Z, Downward J, Futreal PA, Swanton C. Intratumor heterogeneity and branched evolution revealed by multiregion sequencing. *N Engl J Med* 2012; **366**: 883-892 [PMID: 22397650 DOI: 10.1056/NEJMoa1113205]
- 7 Glüer CC, Barkmann R, Hahn HK, Majumdar S, Eckstein F, Nickelsen TN, Bolte H, Dicken V, Heller M. [Parametric biomedical imaging--what defines the quality of quantitative radiological approaches?]. *Röfo* 2006; **178**: 1187-1201 [PMID: 17136644 DOI: 10.1055/s-2006-926973]
- 8 García-Figueiras R, Baleato-González S, Padhani AR, Marhuenda A, Luna A, Alcalá L, Carballo-Castro A, Álvarez-Castro A. Advanced imaging of colorectal cancer: From anatomy to molecular imaging. *Insights Imaging* 2016; **7**: 285-309 [PMID: 27136925 DOI: 10.1007/s13244-016-0465-x]
- 9 Prezzi D, Goh V. Rectal Cancer Magnetic Resonance Imaging: Imaging Beyond Morphology. *Clin Oncol*

- (*R Coll Radiol*) 2016; **28**: 83-92 [PMID: 26586163 DOI: 10.1016/j.clon.2015.10.010]
- 30 **Chun YS**, Vauthey JN, Boonsirikamchai P, Maru DM, Kopetz S, Palavecino M, Curley SA, Abdalla EK, Kaur H, Charnsangavej C, Loyer EM. Association of computed tomography morphology criteria with pathologic response and survival in patients treated with bevacizumab for colorectal liver metastases. *JAMA* 2009; **302**: 2338-2344 [PMID: 19952320 DOI: 10.1001/jama.2009.1755]
  - 31 **Choi H**, Charnsangavej C, Faria SC, Macapinlac HA, Burgess MA, Patel SR, Chen LL, Podoloff DA, Benjamin RS. Correlation of computed tomography and positron emission tomography in patients with metastatic gastrointestinal stromal tumor treated at a single institution with imatinib mesylate: proposal of new computed tomography response criteria. *J Clin Oncol* 2007; **25**: 1753-1759 [PMID: 17470865 DOI: 10.1200/JCO.2006.07.3049]
  - 32 **Lencioni R**, Llovet JM. Modified RECIST (mRECIST) assessment for hepatocellular carcinoma. *Semin Liver Dis* 2010; **30**: 52-60 [PMID: 20175033 DOI: 10.1055/s-0030-1247132]
  - 33 **Rao SX**, Lambregts DM, Schnerr RS, Beckers RC, Maas M, Albarello F, Riedl RG, Dejong CH, Martens MH, Heijnen LA, Backes WH, Beets GL, Zeng MS, Beets-Tan RG. CT texture analysis in colorectal liver metastases: A better way than size and volume measurements to assess response to chemotherapy? *United European Gastroenterol J* 2016; **4**: 257-263 [PMID: 27087955 DOI: 10.1177/2050640615601603]
  - 34 **Shankar S**, Dundamadappa SK, Karam AR, Stay RM, van Sonnenberg E. Imaging of gastrointestinal stromal tumors before and after imatinib mesylate therapy. *Acta Radiol* 2009; **50**: 837-844 [PMID: 19735005 DOI: 10.1080/02841850903059423]
  - 35 **Chung WS**, Park MS, Shin SJ, Baek SE, Kim YE, Choi JY, Kim MJ. Response evaluation in patients with colorectal liver metastases: RECIST version 1.1 versus modified CT criteria. *AJR Am J Roentgenol* 2012; **199**: 809-815 [PMID: 22997372 DOI: 10.2214/AJR.11.7910]
  - 36 **Patterson DM**, Padhani AR, Collins DJ. Technology insight: water diffusion MRI--a potential new biomarker of response to cancer therapy. *Nat Clin Pract Oncol* 2008; **5**: 220-233 [PMID: 18301415 DOI: 10.1038/npcnc1073]
  - 37 **deSouza NM**, Riches SF, Vanas NJ, Morgan VA, Ashley SA, Fisher C, Payne GS, Parker C. Diffusion-weighted magnetic resonance imaging: a potential non-invasive marker of tumour aggressiveness in localized prostate cancer. *Clin Radiol* 2008; **63**: 774-782 [PMID: 18555035 DOI: 10.1016/j.crad.2008.02.001]
  - 38 **Koh DM**, Collins DJ. Diffusion-weighted MRI in the body: applications and challenges in oncology. *AJR Am J Roentgenol* 2007; **188**: 1622-1635 [PMID: 17515386 DOI: 10.2214/AJR.06.1403]
  - 39 **Heijmen L**, Verstappen MC, Ter Voert EE, Punt CJ, Oyen WJ, de Geus-Oei LF, Hermans JJ, Heerschap A, van Laarhoven HW. Tumour response prediction by diffusion-weighted MR imaging: ready for clinical use? *Crit Rev Oncol Hematol* 2012; **83**: 194-207 [PMID: 22269446 DOI: 10.1016/j.critrevonc.2011.12.008]
  - 40 **Rak J**, Mitsuhashi Y, Bayko L, Filmus J, Shirasawa S, Sasazuki T, Kerbel RS. Mutant ras oncogenes upregulate VEGF/VPF expression: implications for induction and inhibition of tumor angiogenesis. *Cancer Res* 1995; **55**: 4575-4580 [PMID: 7553632]
  - 41 **Goh V**, Halligan S, Daley F, Wellsted DM, Guenther T, Bartram CI. Colorectal tumor vascularity: quantitative assessment with multidetector CT--do tumor perfusion measurements reflect angiogenesis? *Radiology* 2008; **249**: 510-517 [PMID: 18812560 DOI: 10.1148/radiol.2492071365]
  - 42 **Goh V**, Glynn-Jones R. Perfusion CT imaging of colorectal cancer. *Br J Radiol* 2014; **87**: 20130811 [PMID: 24434157 DOI: 10.1259/bjr.20130811]
  - 43 **Konerding MA**, Fait E, Gaumann A. 3D microvascular architecture of pre-cancerous lesions and invasive carcinomas of the colon. *Br J Cancer* 2001; **84**: 1354-1362 [PMID: 11355947 DOI: 10.1054/bjoc.2001.1809]
  - 44 **Nelson DA**, Tan TT, Rabson AB, Anderson D, Degenhardt K, White E. Hypoxia and defective apoptosis drive genomic instability and tumorigenesis. *Genes Dev* 2004; **18**: 2095-2107 [PMID: 15314031 DOI: 10.1101/gad.1204904]
  - 45 **O'Connor JP**, Tofts PS, Miles KA, Parkes LM, Thompson G, Jackson A. Dynamic contrast-enhanced imaging techniques: CT and MRI. *Br J Radiol* 2011; **84** Spec No 2: S112-S120 [PMID: 22433822 DOI: 10.1259/bjr/55166688]
  - 46 **Cuenod CA**, Balvay D. Perfusion and vascular permeability: basic concepts and measurement in DCE-CT and DCE-MRI. *Diagn Interv Imaging* 2013; **94**: 1187-1204 [PMID: 24211260 DOI: 10.1016/j.diii.2013.10.010]
  - 47 **Jahng GH**, Li KL, Ostergaard L, Calamante F. Perfusion magnetic resonance imaging: a comprehensive update on principles and techniques. *Korean J Radiol* 2014; **15**: 554-577 [PMID: 25246817 DOI: 10.3348/kjr.2014.15.5.554]
  - 48 **Peller P**, Subramaniam R, Guermazi A, editors. *PET-CT and PET-MRI in Oncology [Internet]*. Berlin, Heidelberg: Springer Berlin Heidelberg; 2012;
  - 49 **Kocael A**, Vatankulu B, Şimşek O, Cengiz M, Kemik A, Kocael P, Halaç M, Sönmezöğlü K, Ulualp K. Comparison of (18)F-fluorodeoxyglucose PET/CT findings with vascular endothelial growth factors and receptors in colorectal cancer. *Tumour Biol* 2016; **37**: 3871-3877 [PMID: 26476536 DOI: 10.1007/s13277-015-4218-0]
  - 50 **Pauwels EK**, Coumou AW, Kostkiewicz M, Kairemo K. [<sup>18</sup>F]fluoro-2-deoxy-d-glucose positron emission tomography/computed tomography imaging in oncology: initial staging and evaluation of cancer therapy. *Med Princ Pract* 2013; **22**: 427-437 [PMID: 23363934 DOI: 10.1159/000346303]
  - 51 **Kilickesmez O**, Atilla S, Soyulu A, Tasdelen N, Bayramoglu S, Cimilli T, Gurmen N. Diffusion-weighted imaging of the rectosigmoid colon: preliminary findings. *J Comput Assist Tomogr* 2009; **33**: 863-866 [PMID: 19940651 DOI: 10.1097/RCT.0b013e31819a60f3]
  - 52 **Jia H**, Ma X, Zhao Y, Zhao J, Liu R, Chen Z, Chen J, Huang J, Li Y, Zhang J, Wang F. Meta-analysis of diffusion-weighted magnetic resonance imaging in identification of colorectal cancer. *Int J Clin Exp Med* 2015; **8**: 17333-17342 [PMID: 26770325]
  - 53 **Curvo-Semedo L**, Lambregts DM, Maas M, Beets GL, Caseiro-Alves F, Beets-Tan RG. Diffusion-weighted MRI in rectal cancer: apparent diffusion coefficient as a potential noninvasive marker of tumor aggressiveness. *J Magn Reson Imaging* 2012; **35**: 1365-1371 [PMID: 22271382 DOI: 10.1002/jmri.23589]
  - 54 **Tong T**, Yao Z, Xu L, Cai S, Bi R, Xin C, Gu Y, Peng W. Extramural depth of tumor invasion at thin-section MR in rectal cancer: associating with prognostic factors and ADC value. *J Magn Reson Imaging* 2014; **40**: 738-744 [PMID: 24307597 DOI: 10.1002/jmri.24398]
  - 55 **Goh V**, Halligan S, Taylor SA, Burling D, Bassett P, Bartram CI. Differentiation between diverticulitis and colorectal cancer: quantitative CT perfusion measurements versus morphologic criteria--initial

- experience. *Radiology* 2007; **242**: 456-462 [PMID: 17255417 DOI: 10.1148/radiol.2422051670]
- 36 **Shen FU**, Lu J, Chen L, Wang Z, Chen Y. Diagnostic value of dynamic contrast-enhanced magnetic resonance imaging in rectal cancer and its correlation with tumor differentiation. *Mol Clin Oncol* 2016; **4**: 500-506 [PMID: 27073650 DOI: 10.3892/mco.2016.762]
- 37 **Sun H**, Xu Y, Yang Q, Wang W. Assessment of tumor grade and angiogenesis in colorectal cancer: whole-volume perfusion CT. *Acad Radiol* 2014; **21**: 750-757 [PMID: 24809317 DOI: 10.1016/j.acra.2014.02.011]
- 38 **Xu Y**, Sun H, Song A, Yang Q, Lu X, Wang W. Predictive Significance of Tumor Grade Using 256-Slice CT Whole-Tumor Perfusion Imaging in Colorectal Adenocarcinoma. *Acad Radiol* 2015; **22**: 1529-1535 [PMID: 26421473 DOI: 10.1016/j.acra.2015.08.023]
- 39 **Oh JR**, Min JJ, Song HC, Chong A, Kim GE, Choi C, Seo JH, Bom HS. A stepwise approach using metabolic volume and SUVmax to differentiate malignancy and dysplasia from benign colonic uptakes on 18F-FDG PET/CT. *Clin Nucl Med* 2012; **37**: e134-e140 [PMID: 22614211 DOI: 10.1097/RLU.0b013e318239245d]
- 40 **van Hooij FB**, Keijsers RG, Loffeld BC, Dun G, Stadhouders PH, Weusten BL. Incidental colonic focal FDG uptake on PET/CT: can the maximum standardized uptake value (SUVmax) guide us in the timing of colonoscopy? *Eur J Nucl Med Mol Imaging* 2015; **42**: 66-71 [PMID: 25139518 DOI: 10.1007/s00259-014-2887-3]
- 41 **Mainenti PP**, Salvatore B, D'Antonio D, De Falco T, De Palma GD, D'Armiento FP, Bucci L, Pace L, Salvatore M. PET/CT colonography in patients with colorectal polyps: a feasibility study. *Eur J Nucl Med Mol Imaging* 2007; **34**: 1594-1603 [PMID: 17492447 DOI: 10.1007/s00259-007-0422-5]
- 42 **Liao CY**, Chen SW, Wu YC, Chen WT, Yen KY, Hsieh TC, Chen PJ, Kao CH. Correlations between 18F-FDG PET/CT parameters and pathological findings in patients with rectal cancer. *Clin Nucl Med* 2014; **39**: e40-e45 [PMID: 24335567 DOI: 10.1097/RLU.0b013e318292f0f6]
- 43 **Mainenti PP**, Cirillo LC, Camera L, Persico F, Cantalupo T, Pace L, De Palma GD, Persico G, Salvatore M. Accuracy of single phase contrast enhanced multidetector CT colonography in the preoperative staging of colo-rectal cancer. *Eur J Radiol* 2006; **60**: 453-459 [PMID: 16965883 DOI: 10.1016/j.ejrad.2006.08.001]
- 44 **Filippone A**, Ambrosini R, Fuschi M, Marinelli T, Genovesi D, Bonomo L. Preoperative T and N staging of colorectal cancer: accuracy of contrast-enhanced multi-detector row CT colonography--initial experience. *Radiology* 2004; **231**: 83-90 [PMID: 14990815 DOI: 10.1148/radiol.2311021152]
- 45 **Kulinna C**, Eibel R, Matzek W, Bonel H, Aust D, Strauss T, Reiser M, Scheidler J. Staging of rectal cancer: diagnostic potential of multiplanar reconstructions with MDCT. *AJR Am J Roentgenol* 2004; **183**: 421-427 [PMID: 15269036 DOI: 10.2214/ajr.183.2.1830421]
- 46 **Brown G**, Richards CJ, Bourne MW, Newcombe RG, Radcliffe AG, Dallimore NS, Williams GT. Morphologic predictors of lymph node status in rectal cancer with use of high-spatial-resolution MR imaging with histopathologic comparison. *Radiology* 2003; **227**: 371-377 [PMID: 12732695 DOI: 10.1148/radiol.2272011747]
- 47 **Mainenti PP**, Iodice D, Segreto S, Storto G, Magliulo M, De Palma GD, Salvatore M, Pace L. Colorectal cancer and 18FDG-PET/CT: what about adding the T to the N parameter in loco-regional staging? *World J Gastroenterol* 2011; **17**: 1427-1433 [PMID: 21472100 DOI: 10.3748/wjg.v17.i11.1427]
- 48 **Heijnen LA**, Lambregts DM, Mondal D, Martens MH, Riedl RG, Beets GL, Beets-Tan RG. Diffusion-weighted MR imaging in primary rectal cancer staging demonstrates but does not characterize lymph nodes. *Eur Radiol* 2013; **23**: 3354-3360 [PMID: 23821022 DOI: 10.1007/s00330-013-2952-5]
- 49 **Lambregts DM**, Maas M, Riedl RG, Bakers FC, Verwoerd JL, Kessels AG, Lammering G, Boetes C, Beets GL, Beets-Tan RG. Value of ADC measurements for nodal staging after chemoradiation in locally advanced rectal cancer—a per lesion validation study. *Eur Radiol* 2011; **21**: 265-273 [PMID: 20730540 DOI: 10.1007/s00330-010-1937-x]
- 50 **Armbruster M**, D'Anastasi M, Holzner V, Kreis ME, Dietrich O, Brandlhuber B, Graser A, Brandlhuber M. Improved detection of a tumorous involvement of the mesorectal fascia and locoregional lymph nodes in locally advanced rectal cancer using DCE-MRI. *Int J Colorectal Dis* 2018; **33**: 901-909 [PMID: 29774398 DOI: 10.1007/s00384-018-3083-x]
- 51 **Grovik E**, Redalen KR, Storås TH, Negård A, Holmedal SH, Ree AH, Meltzer S, Bjørnerud A, Gjesdal KI. Dynamic multi-echo DCE- and DSC-MRI in rectal cancer: Low primary tumor  $K^{trans}$  and  $\Delta R2^*$  peak are significantly associated with lymph node metastasis. *J Magn Reson Imaging* 2017; **46**: 194-206 [PMID: 28001320 DOI: 10.1002/jmri.25566]
- 52 **Yeo DM**, Oh SN, Jung CK, Lee MA, Oh ST, Rha SE, Jung SE, Byun JY, Gall P, Son Y. Correlation of dynamic contrast-enhanced MRI perfusion parameters with angiogenesis and biologic aggressiveness of rectal cancer: Preliminary results. *J Magn Reson Imaging* 2015; **41**: 474-480 [PMID: 24375840 DOI: 10.1002/jmri.24541]
- 53 **Lollert A**, Junginger T, Schimanski CC, Biesterfeld S, Gockel I, Düber C, Oberholzer K. Rectal cancer: dynamic contrast-enhanced MRI correlates with lymph node status and epidermal growth factor receptor expression. *J Magn Reson Imaging* 2014; **39**: 1436-1442 [PMID: 24127411 DOI: 10.1002/jmri.24301]
- 54 **Yang X**, Chen Y, Wen Z, Lu B, Shen B, Xiao X, Yu S. Role of Quantitative Dynamic Contrast-Enhanced MRI in Evaluating Regional Lymph Nodes With a Short-Axis Diameter of Less Than 5 mm in Rectal Cancer. *AJR Am J Roentgenol* 2019; **212**: 77-83 [PMID: 30354269 DOI: 10.2214/AJR.18.19866]
- 55 **Yu XP**, Wen L, Hou J, Wang H, Lu Q. Discrimination of metastatic from non-metastatic mesorectal lymph nodes in rectal cancer using quantitative dynamic contrast-enhanced magnetic resonance imaging. *J Huazhong Univ Sci Technol Med Sci* 2016; **36**: 594-600 [PMID: 27465339 DOI: 10.1007/s11596-016-1631-6]
- 56 **Lu YY**, Chen JH, Ding HJ, Chien CR, Lin WY, Kao CH. A systematic review and meta-analysis of pretherapeutic lymph node staging of colorectal cancer by 18F-FDG PET or PET/CT. *Nucl Med Commun* 2012; **33**: 1127-1133 [PMID: 23000829 DOI: 10.1097/MNM.0b013e328357b2d9]
- 57 **Yi HJ**, Hong KS, Moon N, Chung SS, Lee RA, Kim KH. Reliability of (18)f-fluorodeoxyglucose positron emission tomography/computed tomography in the nodal staging of colorectal cancer patients. *Ann Coloproctol* 2014; **30**: 259-265 [PMID: 25580412 DOI: 10.3393/ac.2014.30.6.259]
- 58 **Tsunoda Y**, Ito M, Fujii H, Kuwano H, Saito N. Preoperative diagnosis of lymph node metastases of colorectal cancer by FDG-PET/CT. *Jpn J Clin Oncol* 2008; **38**: 347-353 [PMID: 18424814 DOI: 10.1093/jjco/hyn032]
- 59 **Yu L**, Tian M, Gao X, Wang D, Qin Y, Geng J. The method and efficacy of 18F-fluorodeoxyglucose positron emission tomography/computed tomography for diagnosing the lymphatic metastasis of colorectal

- carcinoma. *Acad Radiol* 2012; **19**: 427-433 [PMID: 22265721 DOI: 10.1016/j.acra.2011.12.007]
- 60 **Maretto I**, Pomerri F, Pucciarelli S, Mescoli C, Belluco E, Burzi S, Rugge M, Muzzio PC, Nitti D. The potential of restaging in the prediction of pathologic response after preoperative chemoradiotherapy for rectal cancer. *Ann Surg Oncol* 2007; **14**: 455-461 [PMID: 17139456 DOI: 10.1245/s10434-006-9269-4]
- 61 **Chen CC**, Lee RC, Lin JK, Wang LW, Yang SH. How accurate is magnetic resonance imaging in restaging rectal cancer in patients receiving preoperative combined chemoradiotherapy? *Dis Colon Rectum* 2005; **48**: 722-728 [PMID: 15747073 DOI: 10.1007/s10350-004-0851-1]
- 62 **Kuo LJ**, Chern MC, Tsou MH, Liu MC, Jian JJ, Chen CM, Chung YL, Fang WT. Interpretation of magnetic resonance imaging for locally advanced rectal carcinoma after preoperative chemoradiation therapy. *Dis Colon Rectum* 2005; **48**: 23-28 [PMID: 15690653]
- 63 **Joye I**, Deroose CM, Vandecaveye V, Haustermans K. The role of diffusion-weighted MRI and (18)F-FDG PET/CT in the prediction of pathologic complete response after radiochemotherapy for rectal cancer: a systematic review. *Radiother Oncol* 2014; **113**: 158-165 [PMID: 25483833 DOI: 10.1016/j.radonc.2014.11.026]
- 64 **Kim SH**, Lee JM, Gupta SN, Han JK, Choi BI. Dynamic contrast-enhanced MRI to evaluate the therapeutic response to neoadjuvant chemoradiation therapy in locally advanced rectal cancer. *J Magn Reson Imaging* 2014; **40**: 730-737 [PMID: 24307571 DOI: 10.1002/jmri.24387]
- 65 **Lambrecht M**, Vandecaveye V, De Keyzer F, Roels S, Penninckx F, Van Cutsem E, Filip C, Haustermans K. Value of diffusion-weighted magnetic resonance imaging for prediction and early assessment of response to neoadjuvant radiochemotherapy in rectal cancer: preliminary results. *Int J Radiat Oncol Biol Phys* 2012; **82**: 863-870 [PMID: 21398048 DOI: 10.1016/j.ijrobp.2010.12.063]
- 66 **Burbach JP**, den Harder AM, Intven M, van Vulpen M, Verkooijen HM, Reerink O. Impact of radiotherapy boost on pathological complete response in patients with locally advanced rectal cancer: a systematic review and meta-analysis. *Radiother Oncol* 2014; **113**: 1-9 [PMID: 25281582 DOI: 10.1016/j.radonc.2014.08.035]
- 67 **Song I**, Kim SH, Lee SJ, Choi JY, Kim MJ, Rhim H. Value of diffusion-weighted imaging in the detection of viable tumour after neoadjuvant chemoradiation therapy in patients with locally advanced rectal cancer: comparison with T2 weighted and PET/CT imaging. *Br J Radiol* 2012; **85**: 577-586 [PMID: 21343320 DOI: 10.1259/bjr/68424021]
- 68 **Grosu S**, Schäfer AO, Baumann T, Manegold P, Langer M, Gerstmaier A. Differentiating locally recurrent rectal cancer from scar tissue: Value of diffusion-weighted MRI. *Eur J Radiol* 2016; **85**: 1265-1270 [PMID: 27235873 DOI: 10.1016/j.ejrad.2016.04.006]
- 69 **Bassaneze T**, Gonçalves JE, Faria JF, Palma RT, Waisberg J. Quantitative Aspects of Diffusion-weighted Magnetic Resonance Imaging in Rectal Cancer Response to Neoadjuvant Therapy. *Radiol Oncol* 2017; **51**: 270-276 [PMID: 28959163 DOI: 10.1515/raon-2017-0025]
- 70 **Lambrecht M**, Deroose C, Roels S, Vandecaveye V, Penninckx F, Sagaert X, van Cutsem E, de Keyzer F, Haustermans K. The use of FDG-PET/CT and diffusion-weighted magnetic resonance imaging for response prediction before, during and after preoperative chemoradiotherapy for rectal cancer. *Acta Oncol* 2010; **49**: 956-963 [PMID: 20586658 DOI: 10.3109/0284186X.2010.498439]
- 71 **Sun YS**, Zhang XP, Tang L, Ji JF, Gu J, Cai Y, Zhang XY. Locally advanced rectal carcinoma treated with preoperative chemotherapy and radiation therapy: preliminary analysis of diffusion-weighted MR imaging for early detection of tumor histopathologic downstaging. *Radiology* 2010; **254**: 170-178 [PMID: 20019139 DOI: 10.1148/radiol.2541082230]
- 72 **DeVries AF**, Kremser C, Hein PA, Griebel J, Krezcy A, Ofner D, Pfeiffer KP, Lukas P, Judmaier W. Tumor microcirculation and diffusion predict therapy outcome for primary rectal carcinoma. *Int J Radiat Oncol Biol Phys* 2003; **56**: 958-965 [PMID: 12829130]
- 73 **Bellomi M**, Petralia G, Sonzogni A, Zampino MG, Rocca A. CT perfusion for the monitoring of neoadjuvant chemotherapy and radiation therapy in rectal carcinoma: initial experience. *Radiology* 2007; **244**: 486-493 [PMID: 17641369 DOI: 10.1148/radiol.2442061189]
- 74 **Sahani DV**, Kalva SP, Hamberg LM, Hahn PF, Willett CG, Saini S, Mueller PR, Lee TY. Assessing tumor perfusion and treatment response in rectal cancer with multisection CT: initial observations. *Radiology* 2005; **234**: 785-792 [PMID: 15734934 DOI: 10.1148/radiol.2343040286]
- 75 **Curvo-Semedo L**, Portilha MA, Ruivo C, Borrego M, Leite JS, Caseiro-Alves F. Usefulness of perfusion CT to assess response to neoadjuvant combined chemoradiotherapy in patients with locally advanced rectal cancer. *Acad Radiol* 2012; **19**: 203-213 [PMID: 22130088 DOI: 10.1016/j.acra.2011.10.019]
- 76 **Hayano K**, Shuto K, Koda K, Yanagawa N, Okazumi S, Matsubara H. Quantitative measurement of blood flow using perfusion CT for assessing clinicopathologic features and prognosis in patients with rectal cancer. *Dis Colon Rectum* 2009; **52**: 1624-1629 [PMID: 19690492 DOI: 10.1007/DCR.0b013e3181afb79]
- 77 **Hayano K**, Fujishiro T, Sahani DV, Satoh A, Aoyagi T, Ohira G, Tochigi T, Matsubara H, Shuto K. Computed tomography perfusion imaging as a potential imaging biomarker of colorectal cancer. *World J Gastroenterol* 2014; **20**: 17345-17351 [PMID: 25516645 DOI: 10.3748/wjg.v20.i46.17345]
- 78 **Lim JS**, Kim D, Baek SE, Myoung S, Choi J, Shin SJ, Kim MJ, Kim NK, Suh J, Kim KW, Keum KC. Perfusion MRI for the prediction of treatment response after preoperative chemoradiotherapy in locally advanced rectal cancer. *Eur Radiol* 2012; **22**: 1693-1700 [PMID: 22427184 DOI: 10.1007/s00330-012-2416-3]
- 79 **Tong T**, Sun Y, Gollub MJ, Peng W, Cai S, Zhang Z, Gu Y. Dynamic contrast-enhanced MRI: Use in predicting pathological complete response to neoadjuvant chemoradiation in locally advanced rectal cancer. *J Magn Reson Imaging* 2015; **42**: 673-680 [PMID: 25652254 DOI: 10.1002/jmri.24835]
- 80 **Gollub MJ**, Gultekin DH, Akin O, Do RK, Fuqua JL, Gonen M, Kuk D, Weiser M, Saltz L, Schrag D, Goodman K, Paty P, Guillem J, Nash GM, Temple L, Shia J, Schwartz LH. Dynamic contrast enhanced-MRI for the detection of pathological complete response to neoadjuvant chemotherapy for locally advanced rectal cancer. *Eur Radiol* 2012; **22**: 821-831 [PMID: 22101743 DOI: 10.1007/s00330-011-2321-1]
- 81 **Willett CG**, Duda DG, di Tomaso E, Boucher Y, Ancukiewicz M, Sahani DV, Lahdenranta J, Chung DC, Fischman AJ, Lauwers GY, Shellito P, Czitro BG, Wong TZ, Paulson E, Poleski M, Vujaskovic Z, Bentley R, Chen HX, Clark JW, Jain RK. Efficacy, safety, and biomarkers of neoadjuvant bevacizumab, radiation therapy, and fluorouracil in rectal cancer: a multidisciplinary phase II study. *J Clin Oncol* 2009; **27**: 3020-3026 [PMID: 19470921 DOI: 10.1200/JCO.2008.21.1771]
- 82 **Janssen MH**, Öllers MC, van Stiphout RG, Riedl RG, van den Bogaard J, Buijsen J, Lambin P, Lammering G. PET-based treatment response evaluation in rectal cancer: prediction and validation. *Int J*

- Radiat Oncol Biol Phys* 2012; **82**: 871-876 [PMID: 21377810 DOI: 10.1016/j.ijrobp.2010.11.038]
- 83 **Maffione AM**, Chondrogiannis S, Capirci C, Galeotti F, Fornasiero A, Crepaldi G, Grassetto G, Rampin L, Marzola MC, Rubello D. Early prediction of response by <sup>18</sup>F-FDG PET/CT during preoperative therapy in locally advanced rectal cancer: a systematic review. *Eur J Surg Oncol* 2014; **40**: 1186-1194 [PMID: 25060221 DOI: 10.1016/j.ejso.2014.06.005]
- 84 **Rosenberg R**, Herrmann K, Gertler R, Künzli B, Essler M, Lordick F, Becker K, Schuster T, Geinitz H, Maak M, Schwaiger M, Siewert JR, Krause B. The predictive value of metabolic response to preoperative radiochemotherapy in locally advanced rectal cancer measured by PET/CT. *Int J Colorectal Dis* 2009; **24**: 191-200 [PMID: 19050900 DOI: 10.1007/s00384-008-0616-8]
- 85 **Vecchio FM**, Valentini V, Minsky BD, Padula GD, Venkatraman ES, Balducci M, Miccichè F, Ricci R, Morganti AG, Gambacorta MA, Maurizi F, Coco C. The relationship of pathologic tumor regression grade (TRG) and outcomes after preoperative therapy in rectal cancer. *Int J Radiat Oncol Biol Phys* 2005; **62**: 752-760 [PMID: 15936556 DOI: 10.1016/j.ijrobp.2004.11.017]
- 86 **Dworak O**, Keilholz L, Hoffmann A. Pathological features of rectal cancer after preoperative radiochemotherapy. *Int J Colorectal Dis* 1997; **12**: 19-23 [PMID: 9112145]
- 87 **Haberkorn U**, Strauss LG, Dimitrakopoulou A, Engenhart R, Oberdorfer F, Ostertag H, Romahn J, van Kaick G. PET studies of fluorodeoxyglucose metabolism in patients with recurrent colorectal tumors receiving radiotherapy. *J Nucl Med* 1991; **32**: 1485-1490 [PMID: 1714497]
- 88 **Schillaci O**. Use of dual-point fluorodeoxyglucose imaging to enhance sensitivity and specificity. *Semin Nucl Med* 2012; **42**: 267-280 [PMID: 22681676 DOI: 10.1053/j.semnuclmed.2012.02.003]
- 89 **Yoon HJ**, Kim SK, Kim TS, Im HJ, Lee ES, Kim HC, Park JW, Chang HJ, Choi HS, Kim DY, Oh JH. New application of dual point <sup>18</sup>F-FDG PET/CT in the evaluation of neoadjuvant chemoradiation response of locally advanced rectal cancer. *Clin Nucl Med* 2013; **38**: 7-12 [PMID: 23242038 DOI: 10.1097/RLU.0b013e3182639a58]
- 90 **Chow FC**, Chok KS. Colorectal liver metastases: An update on multidisciplinary approach. *World J Hepatol* 2019; **11**: 150-172 [PMID: 30820266 DOI: 10.4254/wjh.v11.i2.150]
- 91 **Mainenti PP**, Mancini M, Mainolfi C, Camera L, Maurea S, Manchia A, Tanga M, Persico F, Addeo P, D'Antonio D, Speranza A, Bucci L, Persico G, Pace L, Salvatore M. Detection of colo-rectal liver metastases: prospective comparison of contrast enhanced US, multidetector CT, PET/CT, and 1.5 Tesla MR with extracellular and reticulo-endothelial cell specific contrast agents. *Abdom Imaging* 2010; **35**: 511-521 [PMID: 19562412 DOI: 10.1007/s00261-009-9555-2]
- 92 **Mainenti PP**, Romano F, Pizzuti L, Segreto S, Storto G, Mannelli L, Imbriaco M, Camera L, Maurea S. Non-invasive diagnostic imaging of colorectal liver metastases. *World J Radiol* 2015; **7**: 157-169 [PMID: 26217455 DOI: 10.4329/wjr.v7.i7.157]
- 93 **Koh DM**, Scurr E, Collins D, Kanber B, Norman A, Leach MO, Husband JE. Predicting response of colorectal hepatic metastasis: value of pretreatment apparent diffusion coefficients. *AJR Am J Roentgenol* 2007; **188**: 1001-1008 [PMID: 17377036 DOI: 10.2214/AJR.06.0601]
- 94 **Cui Y**, Zhang XP, Sun YS, Tang L, Shen L. Apparent diffusion coefficient: potential imaging biomarker for prediction and early detection of response to chemotherapy in hepatic metastases. *Radiology* 2008; **248**: 894-900 [PMID: 18710982 DOI: 10.1148/radiol.2483071407]
- 95 **Coenegrachts K**, Bols A, Haspelslagh M, Rigauts H. Prediction and monitoring of treatment effect using T1-weighted dynamic contrast-enhanced magnetic resonance imaging in colorectal liver metastases: potential of whole tumour ROI and selective ROI analysis. *Eur J Radiol* 2012; **81**: 3870-3876 [PMID: 22944331 DOI: 10.1016/j.ejrad.2012.07.022]
- 96 **Nishioka Y**, Yoshioka R, Gono I, Sugawara T, Yoshida S, Hashimoto M, Shindoh J. Fluorine-18-fluorodeoxyglucose positron emission tomography as an objective substitute for CT morphologic response criteria in patients undergoing chemotherapy for colorectal liver metastases. *Abdom Radiol (NY)* 2018; **43**: 1152-1158 [PMID: 28815337 DOI: 10.1007/s00261-017-1287-0]
- 97 **Brenner H**, Kloor M, Pox CP. Colorectal cancer. *Lancet* 2014; **383**: 1490-1502 [PMID: 24225001 DOI: 10.1016/S0140-6736(13)61649-9]
- 98 **Mahar AL**, Compton C, Halabi S, Hess KR, Weiser MR, Groome PA. Personalizing prognosis in colorectal cancer: A systematic review of the quality and nature of clinical prognostic tools for survival outcomes. *J Surg Oncol* 2017; **116**: 969-982 [PMID: 28767139 DOI: 10.1002/jso.24774]
- 99 **Du CZ**, Xue WC, Cai Y, Li M, Gu J. Lymphovascular invasion in rectal cancer following neoadjuvant radiotherapy: a retrospective cohort study. *World J Gastroenterol* 2009; **15**: 3793-3798 [PMID: 19673022 DOI: 10.3748/wjg.15.3793]
- 100 **Huh JW**, Oh BR, Kim HR, Kim YJ. Preoperative carcinoembryonic antigen level as an independent prognostic factor in potentially curative colon cancer. *J Surg Oncol* 2010; **101**: 396-400 [PMID: 20119979 DOI: 10.1002/jso.21495]
- 101 **Kremser C**, Judmaier W, Hein P, Griebel J, Lukas P, de Vries A. Preliminary results on the influence of chemoradiation on apparent diffusion coefficients of primary rectal carcinoma measured by magnetic resonance imaging. *Strahlenther Onkol* 2003; **179**: 641-649 [PMID: 14628131 DOI: 10.1007/s00066-003-1045-9]
- 102 **Sun Y**, Tong T, Cai S, Bi R, Xin C, Gu Y. Apparent Diffusion Coefficient (ADC) value: a potential imaging biomarker that reflects the biological features of rectal cancer. *PLoS One* 2014; **9**: e109371 [PMID: 25303288 DOI: 10.1371/journal.pone.0109371]
- 103 **Heijmen L**, ter Voert EE, Oyen WJ, Punt CJ, van Spronsen DJ, Heerschap A, de Geus-Oei LF, van Laarhoven HW. Multimodality imaging to predict response to systemic treatment in patients with advanced colorectal cancer. *PLoS One* 2015; **10**: e0120823 [PMID: 25831053 DOI: 10.1371/journal.pone.0120823]
- 104 **Goh V**, Halligan S, Wellsted DM, Bartram CI. Can perfusion CT assessment of primary colorectal adenocarcinoma blood flow at staging predict for subsequent metastatic disease? A pilot study. *Eur Radiol* 2009; **19**: 79-89 [PMID: 18704434 DOI: 10.1007/s00330-008-1128-1]
- 105 **Yu J**, Xu Q, Huang DY, Song JC, Li Y, Xu LL, Shi HB. Prognostic aspects of dynamic contrast-enhanced magnetic resonance imaging in synchronous distant metastatic rectal cancer. *Eur Radiol* 2017; **27**: 1840-1847 [PMID: 27595835 DOI: 10.1007/s00330-016-4532-y]
- 106 **Hirashima Y**, Yamada Y, Tateishi U, Kato K, Miyake M, Horita Y, Akiyoshi K, Takashima A, Okita N, Takahari D, Nakajima T, Hamaguchi T, Shimada Y, Shirao K. Pharmacokinetic parameters from 3-Tesla DCE-MRI as surrogate biomarkers of antitumor effects of bevacizumab plus FOLFIRI in colorectal cancer with liver metastasis. *Int J Cancer* 2012; **130**: 2359-2365 [PMID: 21780098 DOI: 10.1002/ijc.26282]
- 107 **Kim YE**, Joo B, Park MS, Shin SJ, Ahn JB, Kim MJ. Dynamic Contrast-Enhanced Magnetic Resonance

- Imaging as a Surrogate Biomarker for Bevacizumab in Colorectal Cancer Liver Metastasis: A Single-Arm, Exploratory Trial. *Cancer Res Treat* 2016; **48**: 1210-1221 [PMID: 26987390 DOI: 10.4143/crt.2015.374]
- 108 **De Bruyne S**, Van Damme N, Smeets P, Ferdinande L, Ceelen W, Mertens J, Van de Wiele C, Troisi R, Libbrecht L, Laurent S, Geboes K, Peeters M. Value of DCE-MRI and FDG-PET/CT in the prediction of response to preoperative chemotherapy with bevacizumab for colorectal liver metastases. *Br J Cancer* 2012; **106**: 1926-1933 [PMID: 22596235 DOI: 10.1038/bjc.2012.184]
- 109 **Avallone A**, Aloj L, Caracò C, Delrio P, Pecori B, Tatangelo F, Scott N, Casaretti R, Di Gennaro F, Montano M, Silvestro L, Budillon A, Lastoria S. Early FDG PET response assessment of preoperative radiochemotherapy in locally advanced rectal cancer: correlation with long-term outcome. *Eur J Nucl Med Mol Imaging* 2012; **39**: 1848-1857 [PMID: 23053320 DOI: 10.1007/s00259-012-2229-2]
- 110 **Muralidharan V**, Kwok M, Lee ST, Lau L, Scott AM, Christophi C. Prognostic ability of 18F-FDG PET/CT in the assessment of colorectal liver metastases. *J Nucl Med* 2012; **53**: 1345-1351 [PMID: 22797376 DOI: 10.2967/jnumed.112.102749]
- 111 **Lastoria S**, Piccirillo MC, Caracò C, Nasti G, Aloj L, Arrichiello C, de Lutio di Castelguidone E, Tatangelo F, Ottaiano A, Iaffaioli RV, Izzo F, Romano G, Giordano P, Signoriello S, Gallo C, Perrone F. Early PET/CT scan is more effective than RECIST in predicting outcome of patients with liver metastases from colorectal cancer treated with preoperative chemotherapy plus bevacizumab. *J Nucl Med* 2013; **54**: 2062-2069 [PMID: 24136935 DOI: 10.2967/jnumed.113.119909]
- 112 **Lau LF**, Williams DS, Lee ST, Scott AM, Christophi C, Muralidharan V. Metabolic response to preoperative chemotherapy predicts prognosis for patients undergoing surgical resection of colorectal cancer metastatic to the liver. *Ann Surg Oncol* 2014; **21**: 2420-2428 [PMID: 24595797 DOI: 10.1245/s10434-014-3590-0]
- 113 **Gulec SA**, Suthar RR, Barot TC, Pennington K. The prognostic value of functional tumor volume and total lesion glycolysis in patients with colorectal cancer liver metastases undergoing 90Y selective internal radiation therapy plus chemotherapy. *Eur J Nucl Med Mol Imaging* 2011; **38**: 1289-1295 [PMID: 21461737 DOI: 10.1007/s00259-011-1758-4]
- 114 **Giacomobono S**, Gallicchio R, Capacchione D, Nardelli A, Gattozzi D, Lettini G, Molinari L, Mainenti P, Cammarota A, Storto G. F-18 FDG PET/CT in the assessment of patients with unexplained CEA rise after surgical curative resection for colorectal cancer. *Int J Colorectal Dis* 2013; **28**: 1699-1705 [PMID: 23846517 DOI: 10.1007/s00384-013-1747-0]
- 115 **Marcus C**, Wray R, Taghipour M, Marashdeh W, Ahn SJ, Mena E, Subramaniam RM. JOURNAL CLUB: Value of Quantitative FDG PET/CT Volumetric Biomarkers in Recurrent Colorectal Cancer Patient Survival. *AJR Am J Roentgenol* 2016; **207**: 257-265 [PMID: 27447341 DOI: 10.2214/AJR.15.15806]
- 116 **Ogawa S**, Lee TM, Nayak AS, Glynn P. Oxygenation-sensitive contrast in magnetic resonance image of rodent brain at high magnetic fields. *Magn Reson Med* 1990; **14**: 68-78 [PMID: 2161986]
- 117 **Gonçalves MR**, Johnson SP, Ramasawmy R, Pedley RB, Lythgoe MF, Walker-Samuel S. Decomposition of spontaneous fluctuations in tumour oxygenation using BOLD MRI and independent component analysis. *Br J Cancer* 2015; **113**: 1168-1177 [PMID: 26484634 DOI: 10.1038/bjc.2015.270]
- 118 **Chavhan GB**, Babyn PS, Thomas B, Shroff MM, Haacke EM. Principles, techniques, and applications of T2\*-based MR imaging and its special applications. *Radiographics* 2009; **29**: 1433-1449 [PMID: 19755604 DOI: 10.1148/rg.295095034]
- 119 **Padhani AR**, Krohn KA, Lewis JS, Alber M. Imaging oxygenation of human tumours. *Eur Radiol* 2007; **17**: 861-872 [PMID: 17043737 DOI: 10.1007/s00330-006-0431-y]
- 120 **Kim MJ**, Lee SJ, Lee JH, Kim SH, Chun HK, Kim SH, Lim HK, Yun SH. Detection of rectal cancer and response to concurrent chemoradiotherapy by proton magnetic resonance spectroscopy. *Magn Reson Imaging* 2012; **30**: 848-853 [PMID: 22503087 DOI: 10.1016/j.mri.2012.02.013]
- 121 **Wang H**, Wang L, Zhang H, Deng P, Chen J, Zhou B, Hu J, Zou J, Lu W, Xiang P, Wu T, Shao X, Li Y, Zhou Z, Zhao YL. <sup>1</sup>H NMR-based metabolic profiling of human rectal cancer tissue. *Mol Cancer* 2013; **12**: 121 [PMID: 24138801 DOI: 10.1186/1476-4598-12-121]
- 122 **Dzik-Jurasz AS**, Murphy PS, George M, Prock T, Collins DJ, Swift I, Leach MO, Rowland IJ. Human rectal adenocarcinoma: demonstration of 1H-MR spectra in vivo at 1.5 T. *Magn Reson Med* 2002; **47**: 809-811 [PMID: 11948744 DOI: 10.1002/mrm.10108]
- 123 **Ganeshan B**, Miles KA. Quantifying tumour heterogeneity with CT. *Cancer Imaging* 2013; **13**: 140-149 [PMID: 23545171 DOI: 10.1102/1470-7330.2013.0015]
- 124 **Lubner MG**, Smith AD, Sandrasegaran K, Sahani DV, Pickhardt PJ. CT Texture Analysis: Definitions, Applications, Biologic Correlates, and Challenges. *Radiographics* 2017; **37**: 1483-1503 [PMID: 28898189 DOI: 10.1148/rg.2017170056]
- 125 **Aker M**, Ganeshan B, Afaq A, Wan S, Groves AM, Arulampalam T. Magnetic Resonance Texture Analysis in Identifying Complete Pathological Response to Neoadjuvant Treatment in Locally Advanced Rectal Cancer. *Dis Colon Rectum* 2019; **62**: 163-170 [PMID: 30451764 DOI: 10.1097/DCR.0000000000001224]
- 126 **Gillies RJ**, Kinahan PE, Hricak H. Radiomics: Images Are More than Pictures, They Are Data. *Radiology* 2016; **278**: 563-577 [PMID: 26579733 DOI: 10.1148/radiol.2015151169]
- 127 **Stanzione A**, Cuocolo R, Coccozza S, Romeo V, Persico F, Fusco F, Longo N, Brunetti A, Imbriaco M. Detection of Extraprostatic Extension of Cancer on Biparametric MRI Combining Texture Analysis and Machine Learning: Preliminary Results. *Acad Radiol* 2019 [PMID: 30655050 DOI: 10.1016/j.acra.2018.12.025]
- 128 **Romeo V**, Maurea S, Cuocolo R, Petretta M, Mainenti PP, Verde F, Coppola M, Dell'Aversana S, Brunetti A. Characterization of Adrenal Lesions on Unenhanced MRI Using Texture Analysis: A Machine-Learning Approach. *J Magn Reson Imaging* 2018; **48**: 198-204 [PMID: 29341325 DOI: 10.1002/jmri.25954]
- 129 **Mainenti PP**, Romano M, Imbriaco M, Camera L, Pace L, D'Antonio D, Bucci L, Galloro G, Salvatore M. Added value of CT colonography after a positive conventional colonoscopy: impact on treatment strategy. *Abdom Imaging* 2005; **30**: 42-47 [PMID: 15647869 DOI: 10.1007/s00261-004-0246-8]
- 130 **Summers RM**. Polyp size measurement at CT colonography: what do we know and what do we need to know? *Radiology* 2010; **255**: 707-720 [PMID: 20501711 DOI: 10.1148/radiol.10090877]
- 131 **Song B**, Zhang G, Lu H, Wang H, Zhu W, J Pickhardt P, Liang Z. Volumetric texture features from higher-order images for diagnosis of colon lesions via CT colonography. *Int J Comput Assist Radiol Surg* 2014; **9**: 1021-1031 [PMID: 24696313 DOI: 10.1007/s11548-014-0991-2]
- 132 **Liu L**, Liu Y, Xu L, Li Z, Lv H, Dong N, Li W, Yang Z, Wang Z, Jin E. Application of texture analysis

- based on apparent diffusion coefficient maps in discriminating different stages of rectal cancer. *J Magn Reson Imaging* 2017; **45**: 1798-1808 [PMID: 27654307 DOI: 10.1002/jmri.25460]
- 133 **Zhu L**, Pan Z, Ma Q, Yang W, Shi H, Fu C, Yan X, Du L, Yan F, Zhang H. Diffusion Kurtosis Imaging Study of Rectal Adenocarcinoma Associated with Histopathologic Prognostic Factors: Preliminary Findings. *Radiology* 2017; **284**: 66-76 [PMID: 27929929 DOI: 10.1148/radiol.2016160094]
- 134 **Cui C**, Cai H, Liu L, Li L, Tian H, Li L. Quantitative analysis and prediction of regional lymph node status in rectal cancer based on computed tomography imaging. *Eur Radiol* 2011; **21**: 2318-2325 [PMID: 21713526 DOI: 10.1007/s00330-011-2182-7]
- 135 **De Cecco CN**, Ciolina M, Caruso D, Rengo M, Ganeshan B, Meinel FG, Musio D, De Felice F, Tombolini V, Laghi A. Performance of diffusion-weighted imaging, perfusion imaging, and texture analysis in predicting tumoral response to neoadjuvant chemoradiotherapy in rectal cancer patients studied with 3T MR: initial experience. *Abdom Radiol (NY)* 2016; **41**: 1728-1735 [PMID: 27056748 DOI: 10.1007/s00261-016-0733-8]
- 136 **Shu Z**, Fang S, Ye Q, Mao D, Cao H, Pang P, Gong X. Prediction of efficacy of neoadjuvant chemoradiotherapy for rectal cancer: the value of texture analysis of magnetic resonance images. *Abdom Radiol (NY)* 2019 [PMID: 30852633 DOI: 10.1007/s00261-019-01971-y]
- 137 **Palmisano A**, Esposito A, Rancoita PMV, Di Chiara A, Passoni P, Slim N, Campolongo M, Albarello L, Fiorino C, Rosati R, Del Maschio A, De Cobelli F. Could perfusion heterogeneity at dynamic contrast-enhanced MRI be used to predict rectal cancer sensitivity to chemoradiotherapy? *Clin Radiol* 2018; **73**: 911.e1-911.e7 [PMID: 30029837 DOI: 10.1016/j.crad.2018.06.007]
- 138 **Vidal-Vanaclocha F**. The liver prometastatic reaction of cancer patients: implications for microenvironment-dependent colon cancer gene regulation. *Cancer Microenviron* 2011; **4**: 163-180 [PMID: 21870094 DOI: 10.1007/s12307-011-0084-5]
- 139 **Wakai T**, Shirai Y, Sakata J, Kameyama H, Nogami H, Iiai T, Ajioka Y, Hatakeyama K. Histologic evaluation of intrahepatic micrometastases in patients treated with or without neoadjuvant chemotherapy for colorectal carcinoma liver metastasis. *Int J Clin Exp Pathol* 2012; **5**: 308-314 [PMID: 22670174]
- 140 **Rao SX**, Lambregts DM, Schnerr RS, van Ommen W, van Nijnatten TJ, Martens MH, Heijnen LA, Backes WH, Verhoef C, Zeng MS, Beets GL, Beets-Tan RG. Whole-liver CT texture analysis in colorectal cancer: Does the presence of liver metastases affect the texture of the remaining liver? *United European Gastroenterol J* 2014; **2**: 530-538 [PMID: 25452849 DOI: 10.1177/2050640614552463]
- 141 **Zhang H**, Li W, Hu F, Sun Y, Hu T, Tong T. MR texture analysis: potential imaging biomarker for predicting the chemotherapeutic response of patients with colorectal liver metastases. *Abdom Radiol (NY)* 2019; **44**: 65-71 [PMID: 29967982 DOI: 10.1007/s00261-018-1682-1]
- 142 **Ahn SJ**, Kim JH, Park SJ, Han JK. Prediction of the therapeutic response after FOLFOX and FOLFIRI treatment for patients with liver metastasis from colorectal cancer using computerized CT texture analysis. *Eur J Radiol* 2016; **85**: 1867-1874 [PMID: 27666629 DOI: 10.1016/j.ejrad.2016.08.014]
- 143 **Ng F**, Ganeshan B, Kozarski R, Miles KA, Goh V. Assessment of primary colorectal cancer heterogeneity by using whole-tumor texture analysis: contrast-enhanced CT texture as a biomarker of 5-year survival. *Radiology* 2013; **266**: 177-184 [PMID: 23151829 DOI: 10.1148/radiol.12120254]
- 144 **Miles KA**, Ganeshan B, Griffiths MR, Young RC, Chatwin CR. Colorectal cancer: texture analysis of portal phase hepatic CT images as a potential marker of survival. *Radiology* 2009; **250**: 444-452 [PMID: 19164695 DOI: 10.1148/radiol.2502071879]
- 145 **Lovinfosse P**, Polus M, Van Daele D, Martinive P, Daenen F, Hatt M, Visvikis D, Koopmansch B, Lambert F, Coimbra C, Seidel L, Albert A, Delvenne P, Hustinx R. FDG PET/CT radiomics for predicting the outcome of locally advanced rectal cancer. *Eur J Nucl Med Mol Imaging* 2018; **45**: 365-375 [PMID: 29046927 DOI: 10.1007/s00259-017-3855-5]
- 146 **Martens MH**, van Heeswijk MM, van den Broek JJ, Rao SX, Vandecaveye V, Vliegen RA, Schreurs WH, Beets GL, Lambregts DM, Beets-Tan RG. Prospective, Multicenter Validation Study of Magnetic Resonance Volumetry for Response Assessment After Preoperative Chemoradiation in Rectal Cancer: Can the Results in the Literature be Reproduced? *Int J Radiat Oncol Biol Phys* 2015; **93**: 1005-1014 [PMID: 26581139 DOI: 10.1016/j.ijrobp.2015.09.008]
- 147 **Neri E**, Guidi E, Pancrazi F, Castagna M, Castelluccio E, Balestri R, Buccianti P, Masi L, Falcone A, Manfredi B, Faggioni L, Bartolozzi C. MRI tumor volume reduction rate vs tumor regression grade in the pre-operative re-staging of locally advanced rectal cancer after chemo-radiotherapy. *Eur J Radiol* 2015; **84**: 2438-2443 [PMID: 26462793 DOI: 10.1016/j.ejrad.2015.08.008]
- 148 **Atasoy G**, Arslan NC, Elibol FD, Sagol O, Obuz F, Sokmen S. Magnetic resonance-based pelvimetry and tumor volumetry can predict surgical difficulty and oncologic outcome in locally advanced mid-low rectal cancer. *Surg Today* 2018; **48**: 1040-1051 [PMID: 29961173 DOI: 10.1007/s00595-018-1690-3]
- 149 **Okuno T**, Kawai K, Koyama K, Takahashi M, Ishihara S, Momose T, Morikawa T, Fukayama M, Watanabe T. Value of FDG-PET/CT Volumetry After Chemoradiotherapy in Rectal Cancer. *Dis Colon Rectum* 2018; **61**: 320-327 [PMID: 29360680 DOI: 10.1097/DCR.0000000000000959]
- 150 **Pomerri F**, Pucciarelli S, Gennaro G, Maretto I, Nitti D, Muzzio PC. Comparison between CT volume measurement and histopathological assessment of response to neoadjuvant therapy in rectal cancer. *Eur J Radiol* 2012; **81**: 3918-3924 [PMID: 22902408 DOI: 10.1016/j.ejrad.2012.04.038]
- 151 **Kim S**, Han K, Seo N, Kim HJ, Kim MJ, Koom WS, Ahn JB, Lim JS. T2-weighted signal intensity-selected volumetry for prediction of pathological complete response after preoperative chemoradiotherapy in locally advanced rectal cancer. *Eur Radiol* 2018; **28**: 5231-5240 [PMID: 29858637 DOI: 10.1007/s00330-018-5520-1]
- 152 **Gollub MJ**, Hotker AM, Woo KM, Mazaheri Y, Gonen M. Quantitating whole lesion tumor biology in rectal cancer MRI: taking a lesson from FDG-PET tumor metrics. *Abdom Radiol (NY)* 2018; **43**: 1575-1582 [PMID: 29159523 DOI: 10.1007/s00261-017-1389-8]
- 153 **Koh TS**, Ng QS, Thng CH, Kwek JW, Kozarski R, Goh V. Primary colorectal cancer: use of kinetic modeling of dynamic contrast-enhanced CT data to predict clinical outcome. *Radiology* 2013; **267**: 145-154 [PMID: 23297334 DOI: 10.1148/radiol.12120186]
- 154 **Hakimé A**, Peddi H, Hines-Peralta AU, Wilcox CJ, Kruskal J, Lin S, de Baere T, Raptopoulos VD, Goldberg SN. CT perfusion for determination of pharmacologically mediated blood flow changes in an animal tumor model. *Radiology* 2007; **243**: 712-719 [PMID: 17517930 DOI: 10.1148/radiol.2433052048]
- 155 **van Laarhoven HW**, de Geus-Oei LF, Wiering B, Lok J, Rijpkema M, Kaanders JH, Krabbe PF, Ruers T, Punt CJ, van der Kogel AJ, Oyen WJ, Heerschap A. Gadopentetate dimeglumine and FDG uptake in liver metastases of colorectal carcinoma as determined with MR imaging and PET. *Radiology* 2005; **237**: 181-188 [PMID: 16183932 DOI: 10.1148/radiol.2371041397]

- 156 **Goh V**, Engledow A, Rodriguez-Justo M, Shastry M, Peck J, Blackman G, Endozo R, Taylor S, Halligan S, Ell P, Groves AM. The flow-metabolic phenotype of primary colorectal cancer: assessment by integrated 18F-FDG PET/perfusion CT with histopathologic correlation. *J Nucl Med* 2012; **53**: 687-692 [PMID: 22454485 DOI: 10.2967/jnumed.111.098525]
- 157 **Janssen MH**, Aerts HJ, Buijsen J, Lambin P, Lammering G, Öllers MC. Repeated positron emission tomography-computed tomography and perfusion-computed tomography imaging in rectal cancer: fluorodeoxyglucose uptake corresponds with tumor perfusion. *Int J Radiat Oncol Biol Phys* 2012; **82**: 849-855 [PMID: 21392896 DOI: 10.1016/j.ijrobp.2010.10.029]
- 158 **Gu J**, Khong PL, Wang S, Chan Q, Wu EX, Law W, Liu RK, Zhang J. Dynamic contrast-enhanced MRI of primary rectal cancer: quantitative correlation with positron emission tomography/computed tomography. *J Magn Reson Imaging* 2011; **33**: 340-347 [PMID: 21274975 DOI: 10.1002/jmri.22405]
- 159 **Fischer MA**, Vrugt B, Alkadhi H, Hahnloser D, Hany TF, Veit-Haibach P. Integrated 18F-FDG PET/perfusion CT for the monitoring of neoadjuvant chemoradiotherapy in rectal carcinoma: correlation with histopathology. *Eur J Nucl Med Mol Imaging* 2014; **41**: 1563-1573 [PMID: 24760269 DOI: 10.1007/s00259-014-2752-4]
- 160 **Wu J**, Tha KK, Xing L, Li R. Radiomics and radiogenomics for precision radiotherapy. *J Radiat Res* 2018; **59**: i25-i31 [PMID: 29385618 DOI: 10.1093/jrr/rrx102]
- 161 **García-Figueiras R**, Baleato-González S, Padhani AR, Luna-Alcalá A, Marhuenda A, Vilanova JC, Osorio-Vázquez I, Martínez-de-Alegria A, Gómez-Caamaño A. Advanced Imaging Techniques in Evaluation of Colorectal Cancer. *Radiographics* 2018; **38**: 740-765 [PMID: 29676964 DOI: 10.1148/rg.2018170044]
- 162 **Horvat N**, Veeraraghavan H, Pelossof RA, Fernandes MC, Arora A, Khan M, Marco M, Cheng CT, Gonen M, Golia Pernicka JS, Gollub MJ, Garcia-Aguillar J, Petkovska I. Radiogenomics of rectal adenocarcinoma in the era of precision medicine: A pilot study of associations between qualitative and quantitative MRI imaging features and genetic mutations. *Eur J Radiol* 2019; **113**: 174-181 [PMID: 30927944 DOI: 10.1016/j.ejrad.2019.02.022]
- 163 **Shin YR**, Kim KA, Im S, Hwang SS, Kim K. Prediction of KRAS Mutation in Rectal Cancer Using MRI. *Anticancer Res* 2016; **36**: 4799-4804 [PMID: 27630331 DOI: 10.21873/anticancer.11039]
- 164 **Mao W**, Zhou J, Zhang H, Qiu L, Tan H, Hu Y, Shi H. Relationship between KRAS mutations and dual time point <sup>18</sup>F-FDG PET/CT imaging in colorectal liver metastases. *Abdom Radiol (NY)* 2019; **44**: 2059-2066 [PMID: 30143816 DOI: 10.1007/s00261-018-1740-8]
- 165 **Chen SW**, Chiang HC, Chen WT, Hsieh TC, Yen KY, Chiang SF, Kao CH. Correlation between PET/CT parameters and KRAS expression in colorectal cancer. *Clin Nucl Med* 2014; **39**: 685-689 [PMID: 24978328 DOI: 10.1097/RLU.0000000000000481]
- 166 **Miles KA**, Ganeshan B, Rodriguez-Justo M, Goh VJ, Ziauddin Z, Engledow A, Meagher M, Endozo R, Taylor SA, Halligan S, Ell PJ, Groves AM. Multifunctional imaging signature for V-KI-RAS2 Kirsten rat sarcoma viral oncogene homolog (KRAS) mutations in colorectal cancer. *J Nucl Med* 2014; **55**: 386-391 [PMID: 24516257 DOI: 10.2967/jnumed.113.120485]





Published By Baishideng Publishing Group Inc  
7041 Koll Center Parkway, Suite 160, Pleasanton, CA 94566, USA  
Telephone: +1-925-2238242  
E-mail: [bpgoffice@wjgnet.com](mailto:bpgoffice@wjgnet.com)  
Help Desk: <http://www.f6publishing.com/helpdesk>  
<http://www.wjgnet.com>

